4TH IDPASC SCHOOL

Braga, 20 - 28 January 2014

CMB and Galaxy Clusters at Planck frequencies

António da Silva
DF-FCUL

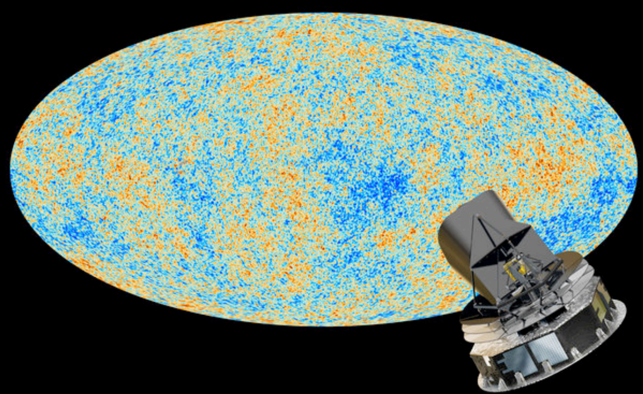

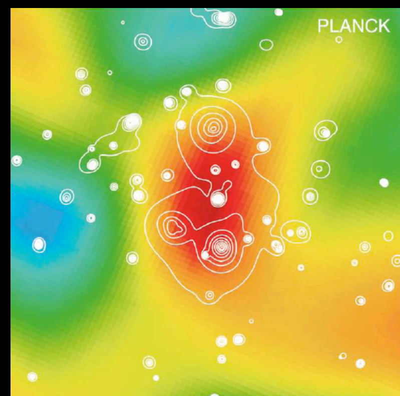

Fig. credits: ESA and the Planck collaboration

Syllabus:

Outline: This course provides a short introduction to the Cosmic Microwave Background (CMB) radiation and Galaxy clusters as probes of Cosmology and Large Scale Structure (LSS). After briefly reviewing the current standard model of cosmology, we will describe the main properties of the CMB and Sunyaev-Zeld'ovich (SZ) clusters and finalize with an overview of the latest findings obtained with the Planck satellite (ESA).

Contents:

Part 1: Review of the Standard Model of Cosmology (SMC):
Part 2: CMB and Sunyaev-Zel'dovich (SZ) Galaxy Clusters
Part 3: Latest results from the Planck Satellite

Bibliography:

- Primordial cosmology, P. Peter, J.-P. Uzan, Oxford University Press, 2009
- An Introduction to Modern Cosmology, A. Liddle, J. Wiley & Sons, 2003
- Course notes by the module's responsible

Part II: CMB and Sunyaev-Zel’dovich (SZ) effect in Galaxy Clusters

Microwave spectral region

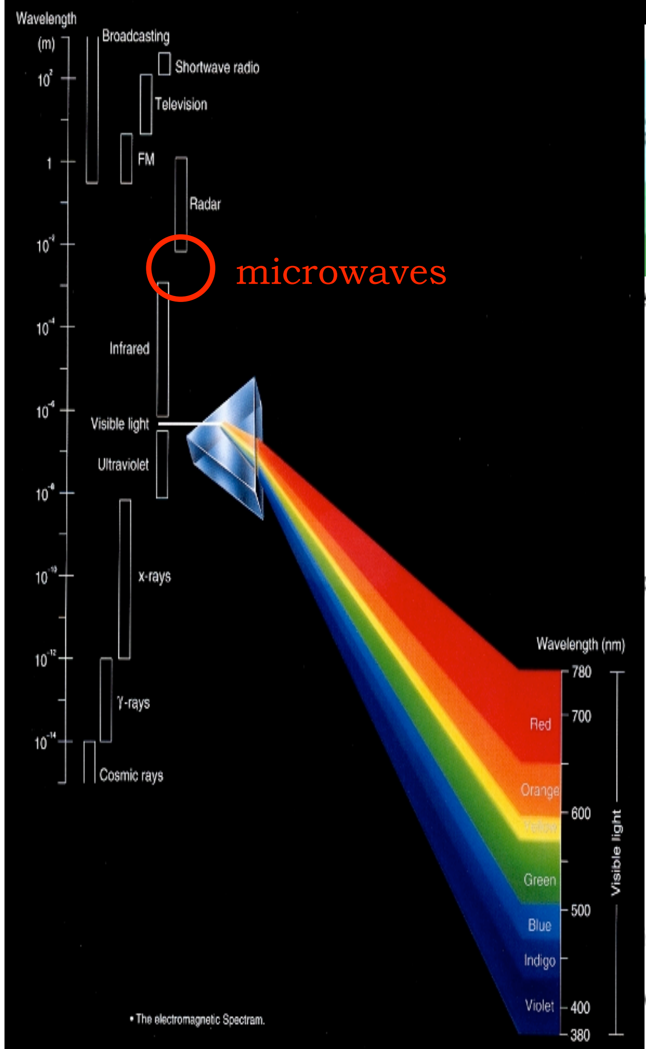

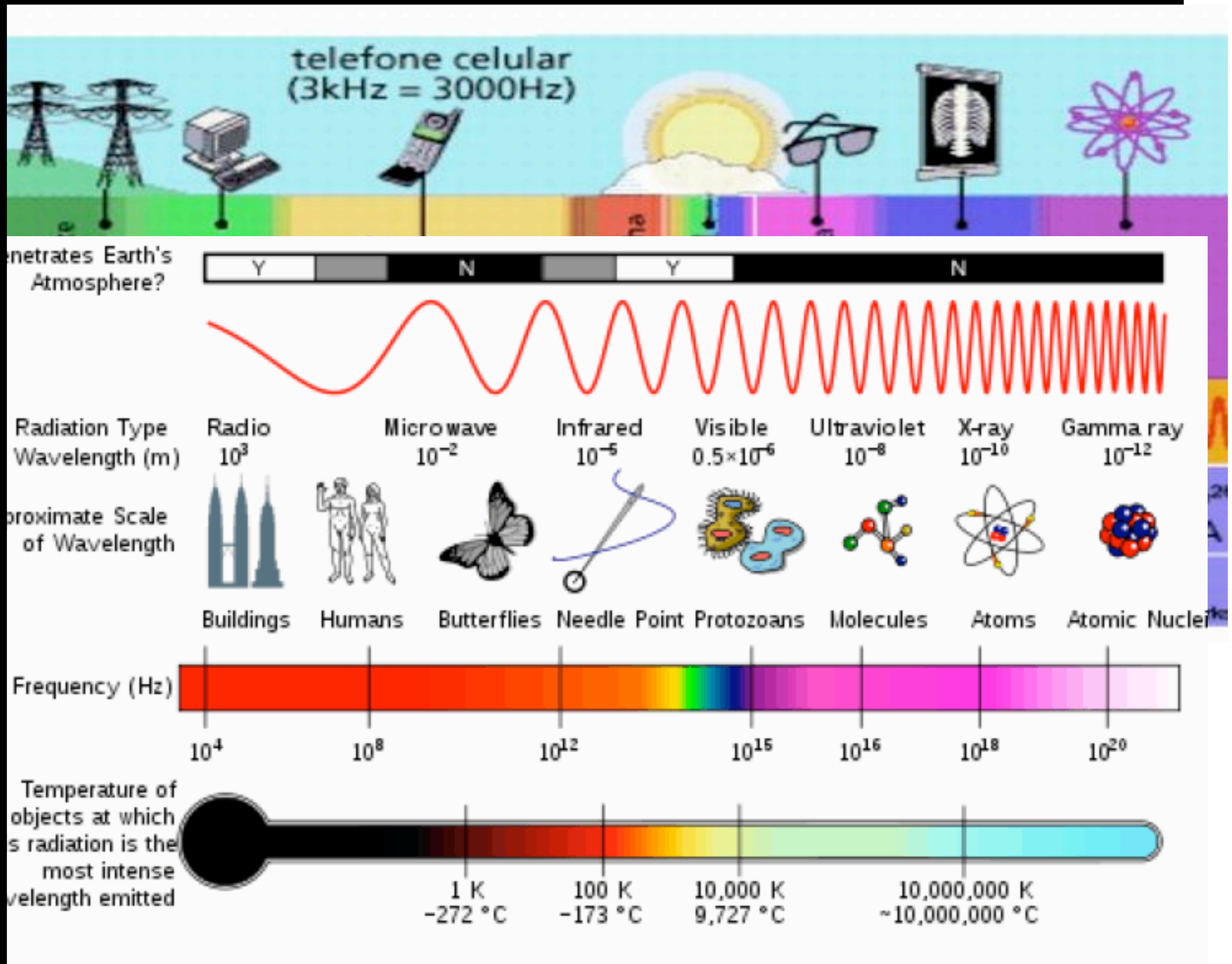

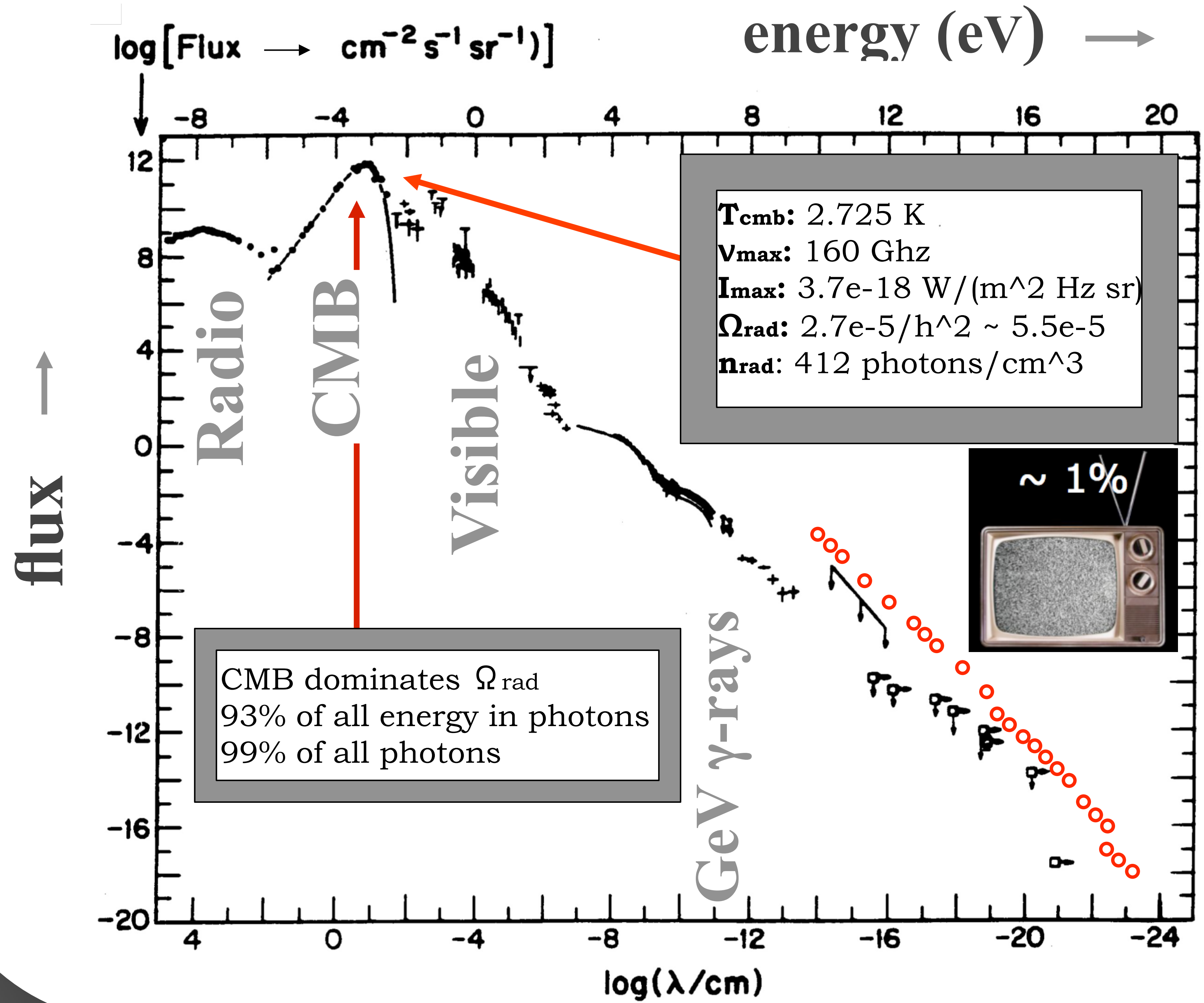
log[Flux → cm^-2 s^-1 sr^-1)]
energy (eV)
-8 -4 0 4 8 12 16 20
12 8 4 0 -4 -8 -12 -16 -20
flux
Radio
CMB
Visible
GeV γ-rays
Tcmb: 2.725 K
Vmax: 160 Ghz
Imax: 3.7e-18 W/(m^2 Hz sr)
Ωrad: 2.7e-5/h^2 ~ 5.5e-5
nrad: 412 photons/cm^3
~ 1%
CMB dominates Ω rad
93% of all energy in photons
99% of all photons
4 0 -4 -8 -12 -16 -20 -24
log(λ/cm)

Cosmic Microwave Background

Penzias & Wilson

1965: Penzias & Wilson serendipitously discovered a uniform radiation ("excess") across the sky.

This was the cosmic microwave background radiation predicted by Gamow and Alpher in 1948

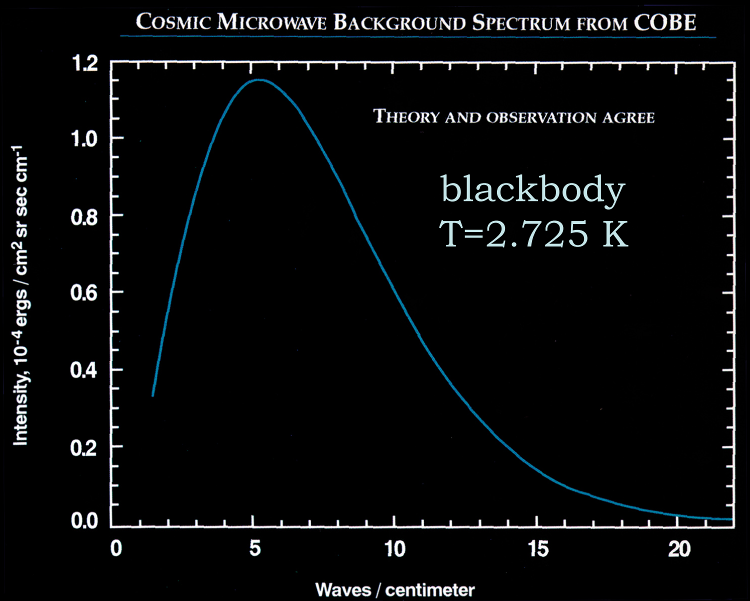

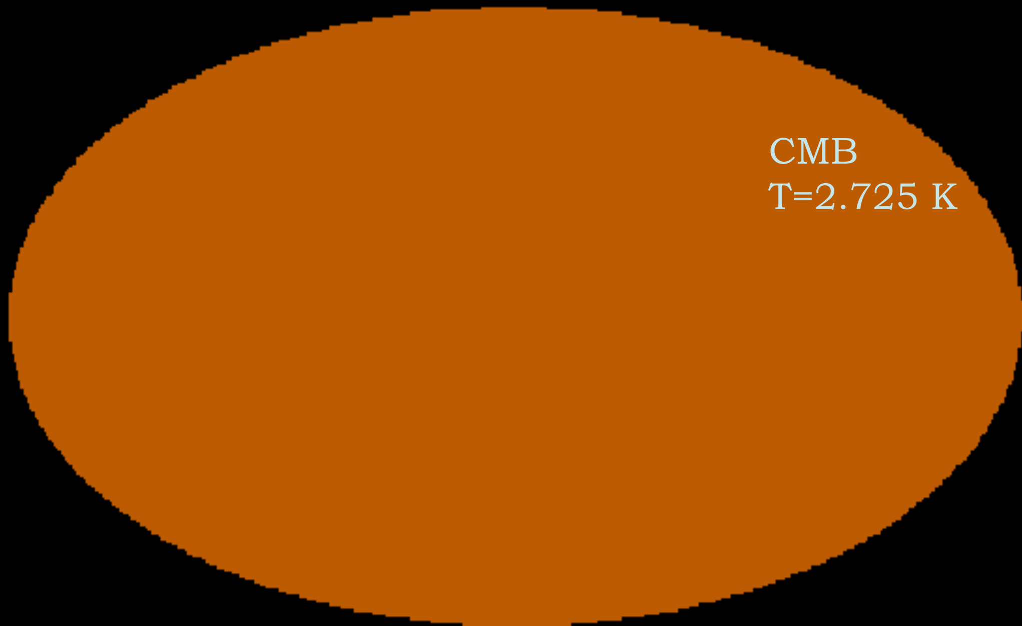

Cosmic Microwave Background

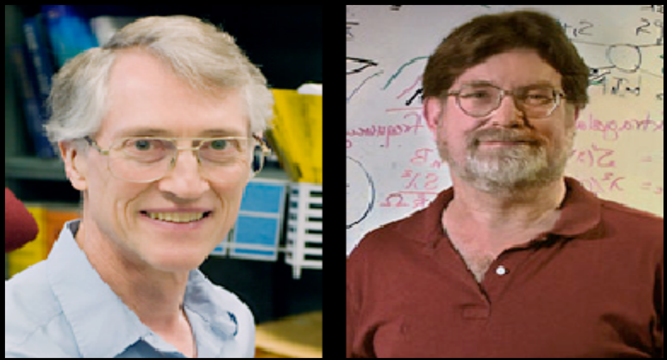

John Matter &
Geroge Smooth

1991: High precision measurement of CMB temperature by COBE and 1st detection of temperature fluctuations (Mather & Smoot)

2001: State of the art measurements of dT/T~1e-5 temperature fluctuations by WMAP

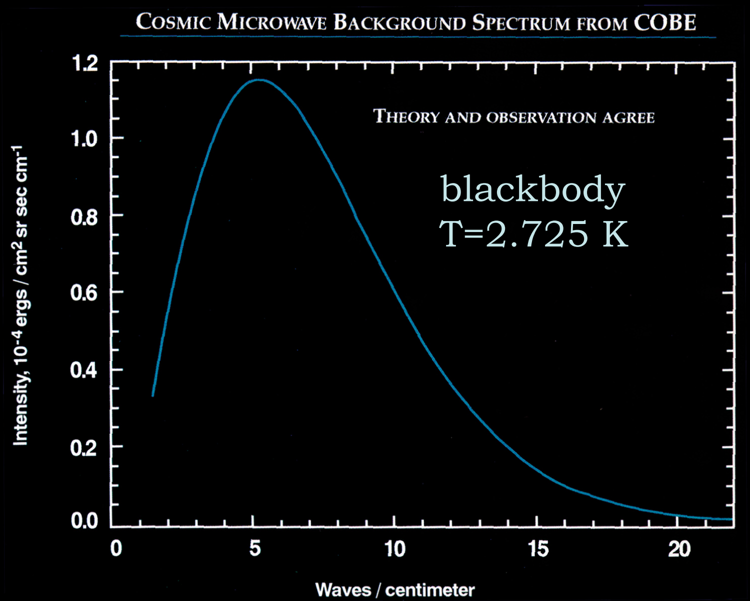

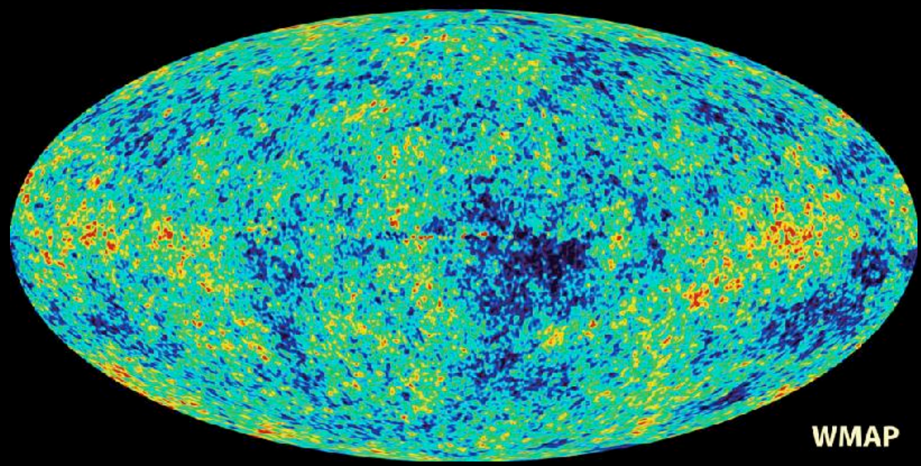

Fig. credits: NASA / WMAP Science Team

CMB: a snapshot at the time of decoupling (z ~1100)

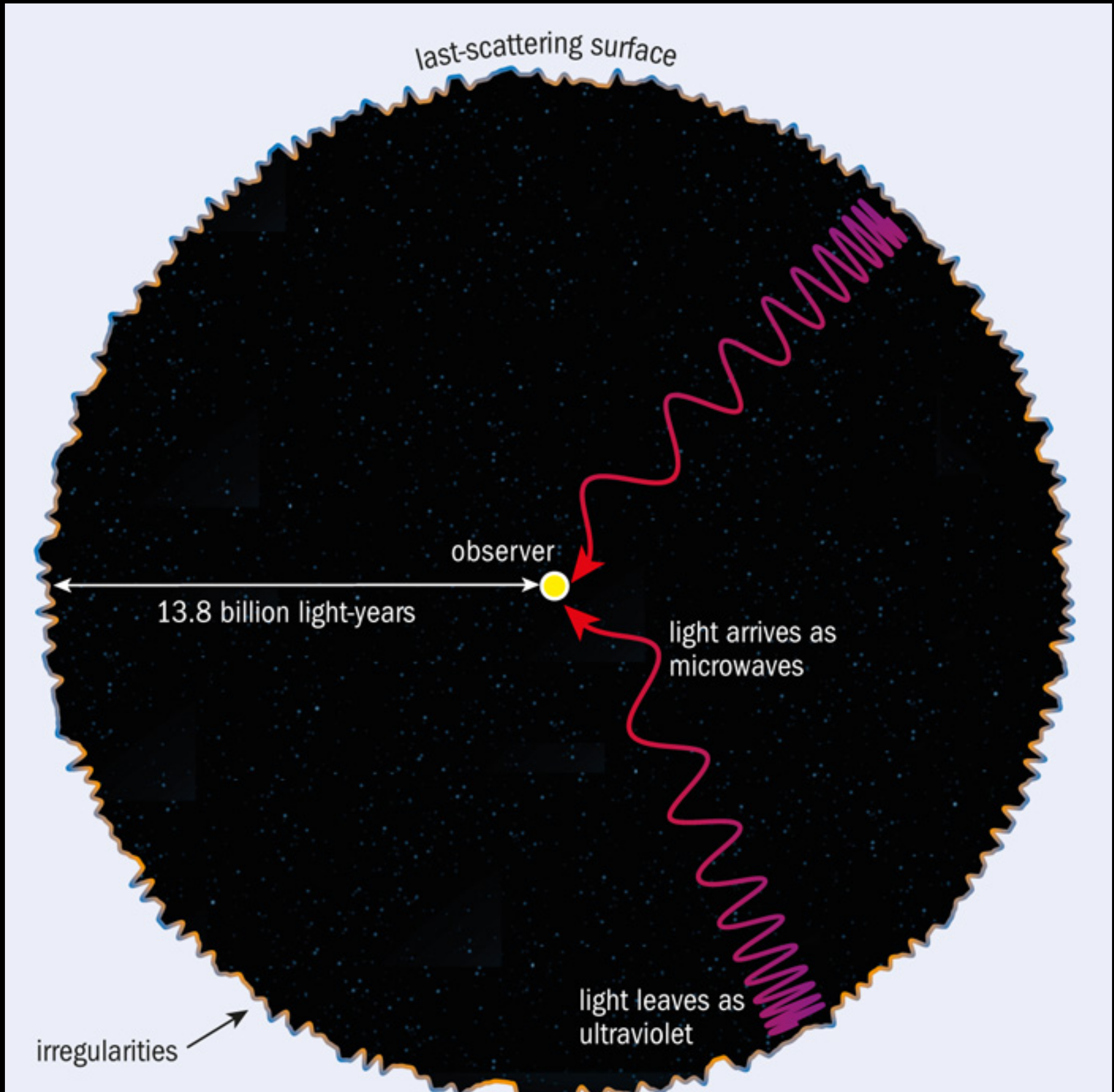

Reprinted from: http://physicsworld.com/cws/article/indepth/2014/jan/09/planck-perspectives


CMB analogy with a cloudy sky
Distance: ~km

CMB: a snapshot at the time of decoupling

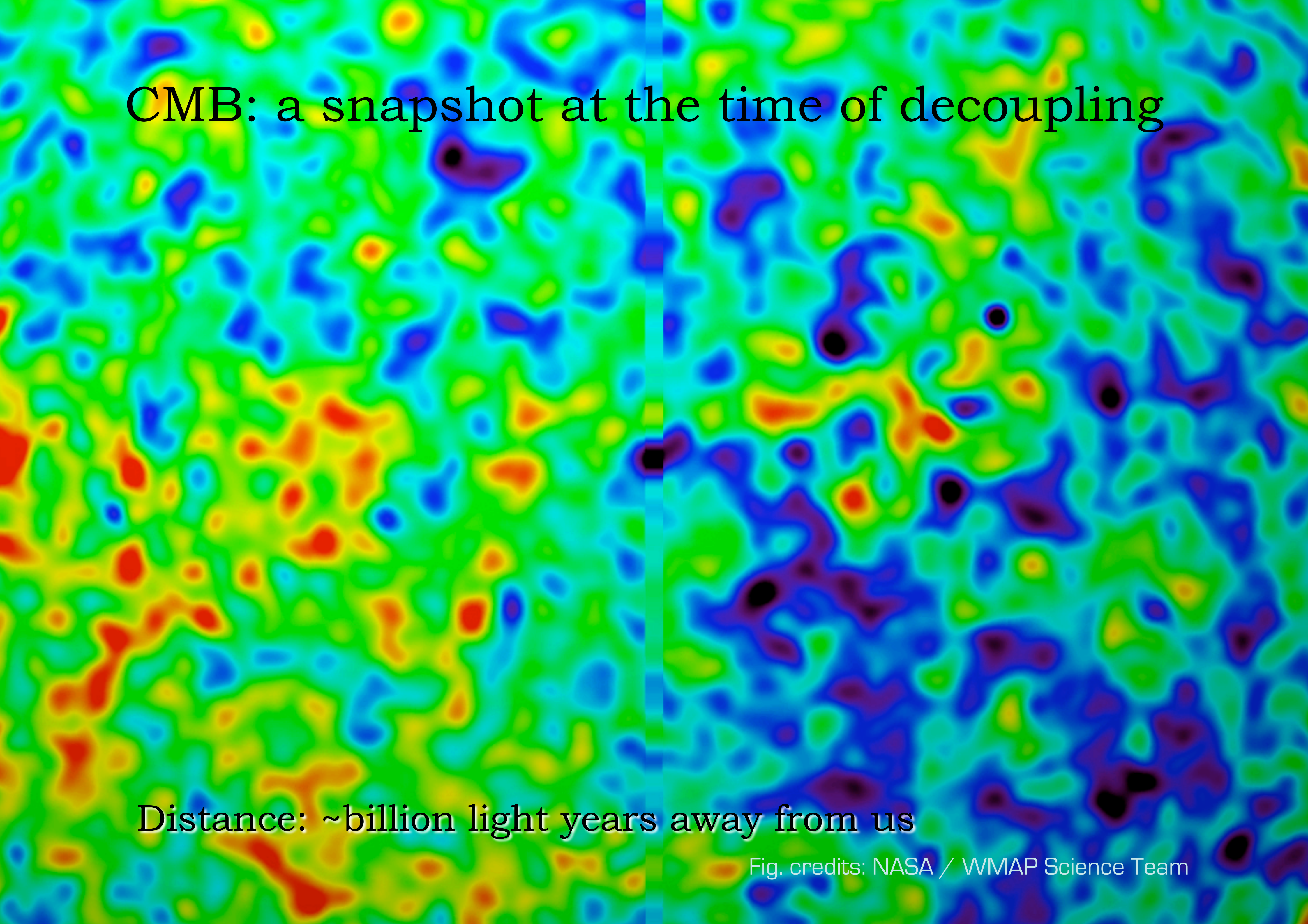

Distance: ~billion light years away from us

Fig. credits: NASA / WMAP Science Team

Decoupling

It can be defined as when the number of photon-baryon interactions falls below 1

$$N_{int} = \int_{t_i}^{\infty} \Gamma_{int}(t)dt$$

where the interaction rate (v=c) is

$$\Gamma_{int} = n\sigma|\vec{v}|$$

The photons mean free path tend to infinity

$$\lambda_\gamma \simeq \Gamma_\gamma^{-1}(\Omega_B h^2)$$

with

$$\Gamma_\gamma = n_e\sigma_T$$

$$\sigma_T = 6.65 \times 10^{-25}\ \mathrm{cm}^2$$

Recombination

As the Universe expands the ionization fraction

$$X_e^{eq} = n_e/(n_p + n_H)$$

$$e^- + p \rightleftharpoons H + \gamma$$

decreases, according to the Saha equation

$$\frac{1 - X_e^{eq}}{(X_e^{eq})^2} = \frac{4\sqrt{2}\zeta(3)}{\sqrt{\pi}}\eta\left(\frac{T}{m_e}\right)^{3/2}\exp(B/T)$$

where,

- B electron biding energy

$$B = (m_p + m_e - m_H)c^2 = 13.6eV$$

- η baryon – photon ratio (~1e–10)

$$\eta\,(t_0) = \frac{n_B\,(t_0)}{n_\gamma\,(t_0)} = 2.74 \times 10^{-8}\,\Omega_B h^2$$

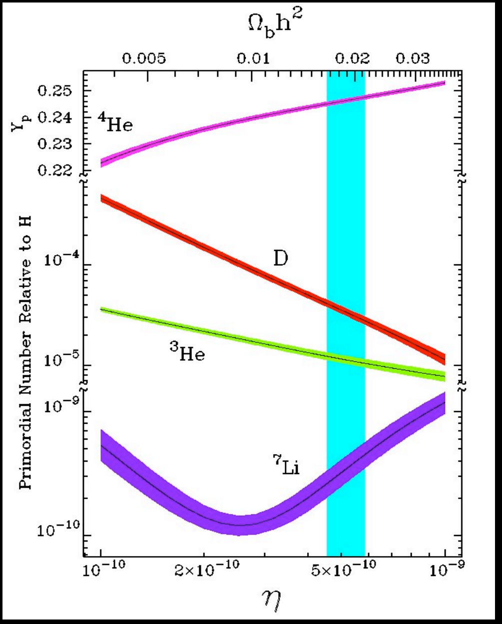

Recombination versus Decoupling

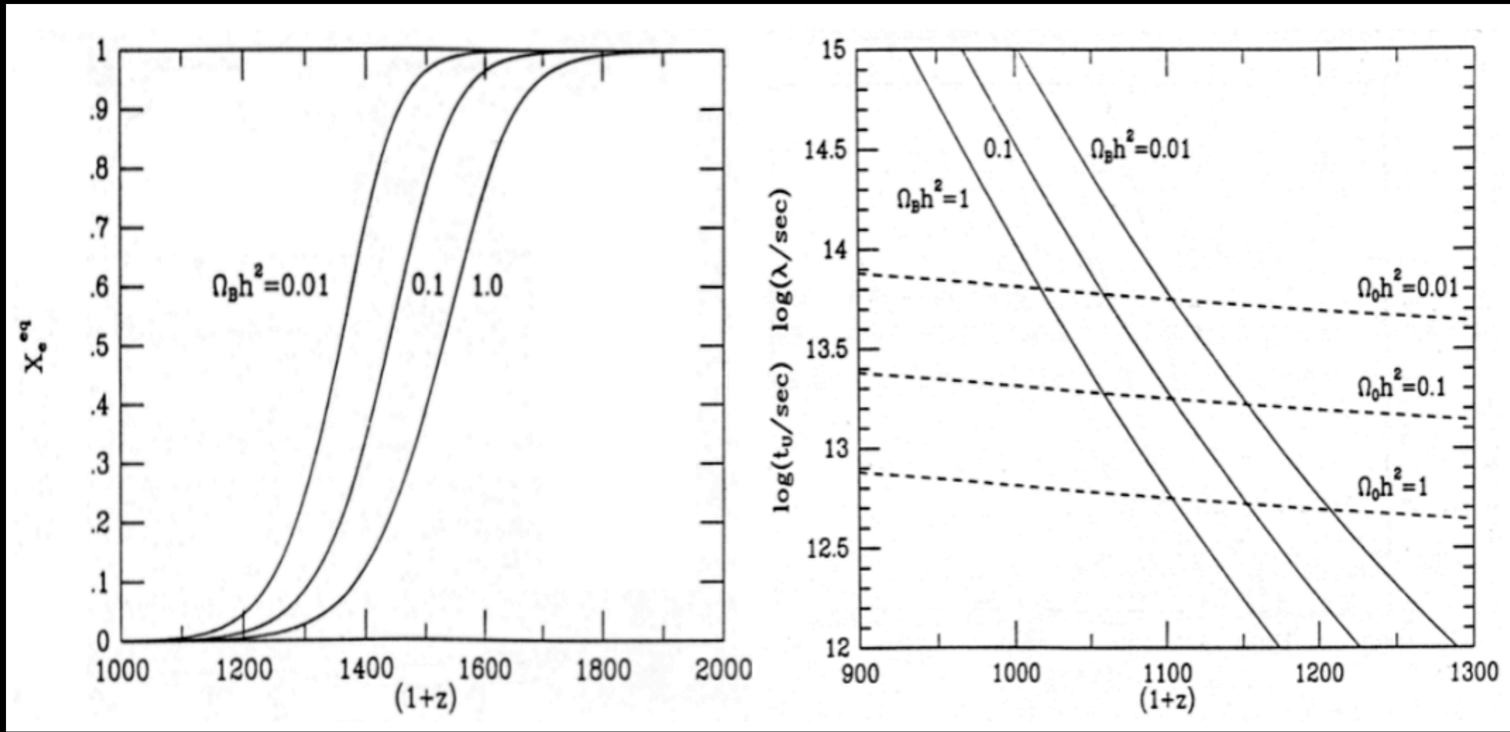

Assuming recombination as when ionization faction fall below 10% we have:

Time of recombination

$$
\begin{aligned}
z_{rec} &= z(t_{rec}) \simeq 1200 - 1400 \\
T_{rec} &= T(t_{rec}) \simeq 3274 - 3819\,K = 0.28 - 0.33\,eV \\
t_{rec} &\simeq (125 - 157) \times 10^3 \left(\Omega_0 h^2\right)^{-1/2} \; anos.
\end{aligned}
$$

Time of CMB decoupling

$$
\begin{aligned}
z_{dec} &= z(t_{dec}) \simeq 1100 \\
T_{dec} &= T(t_{dec}) \simeq 3000\,K = 0.26\,eV \\
t_{dec} &\simeq 179 \times 10^3 \left(\Omega_0 h^2\right)^{-1/2} \; anos.
\end{aligned}
$$

The intensity spectrum and polarization of the CMB

CMB intensity spectrum

Why the CMB has black body spectrum?

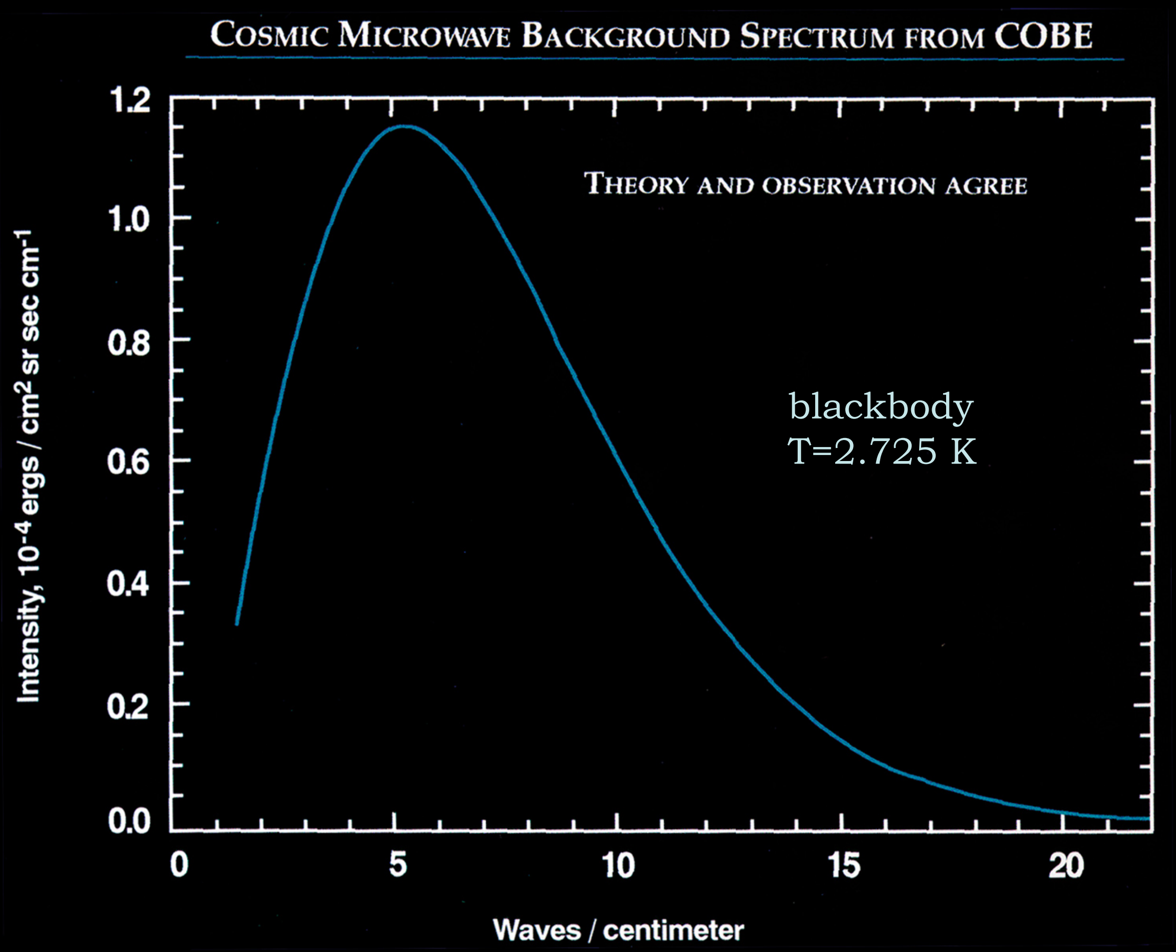

CMB intensity spectrum

Why the CMB has black body spectrum?

- the shape of CMB spectrum depends on interactions between matter and radiation. After z~1.000.000.000 (particle – anti-particle annihilation) the main physical processes are:

  - Compton scattering:
    able to guarantee kinetic equilibrium (Bose-Einstein spectrum) down to: $z_c \sim 300.000$ ($1e9 < z_c < 3e5$)

$$I(\nu) = \frac{2h\nu^3}{c^2}\left[\exp\left(\frac{h\nu}{k_B T} + \mu(\nu)\right) - 1\right]^{-1}$$

  - double Compton scattering
    able to generate thermal equilibrium (black body spectrum) down to: $z_{th} \sim 2.000.000$ ($1e9 < z_{th} < 2e6$)

  - free-free (Bremsstrahlung) emission
    also contributes to generate thermal equilibrium

CMB intensity spectrum

Why the CMB has black body spectrum?

the CMB acquires a blackbody spectrum due to matter-radiation interactions by z_{th} ~ 2e6

• if physical processes release energy between $z_{th} < z < z_c$ (2.000.000 < z < 300.000) the CMB acquires a Bose-Einstein spectrum

• energy releases after z_c ~ 300.000 will distort the CMB spectrum (as in the case of the SZ effect, Line emission, non-standard physics…)

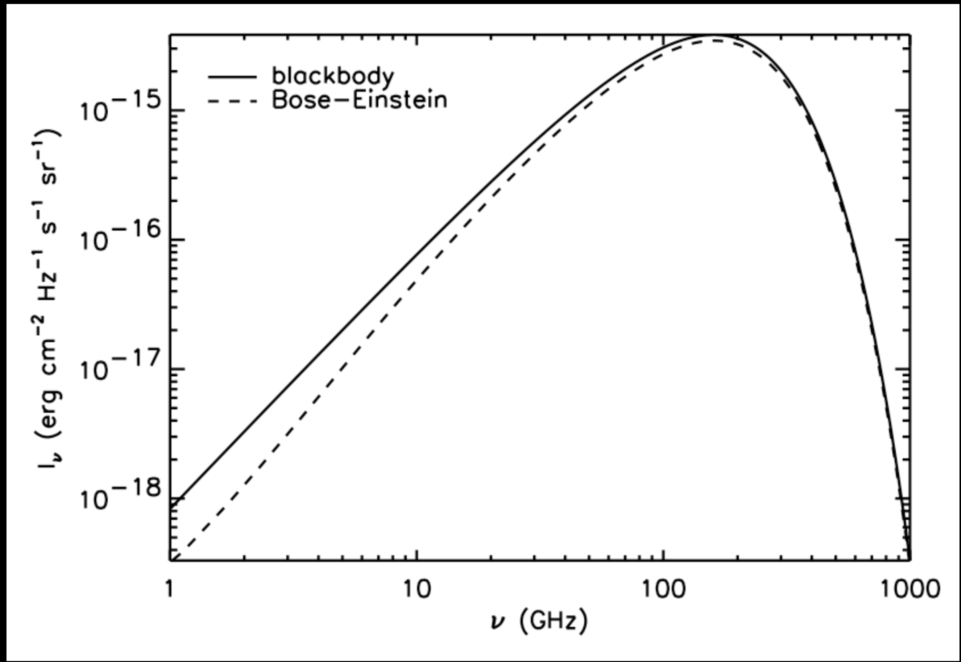

COBE-FIRAS: spectral deviations from a blackbody are very small: $|\mu| < 9$ e-5

Refs: Peebles, Physical Cosmology, Cambridge U.P., 1991; Burigana et al. A&A, 1991, 246, 49

CMB intensity spectrum

Why the CMB has black body spectrum?

the CMB acquires a blackbody spectrum due to matter-radiation interactions by z_{th} ~ 2e6

• if physical processes release energy between $z_{th} < z < z_c$ (2.000.000 < z < 300.000) the CMB acquires a Bose-Einstein spectrum

• energy releases after z_c ~ 300.000 will distort the CMB spectrum (as in the case of the SZ effect, Line emission, non-standard physics…)

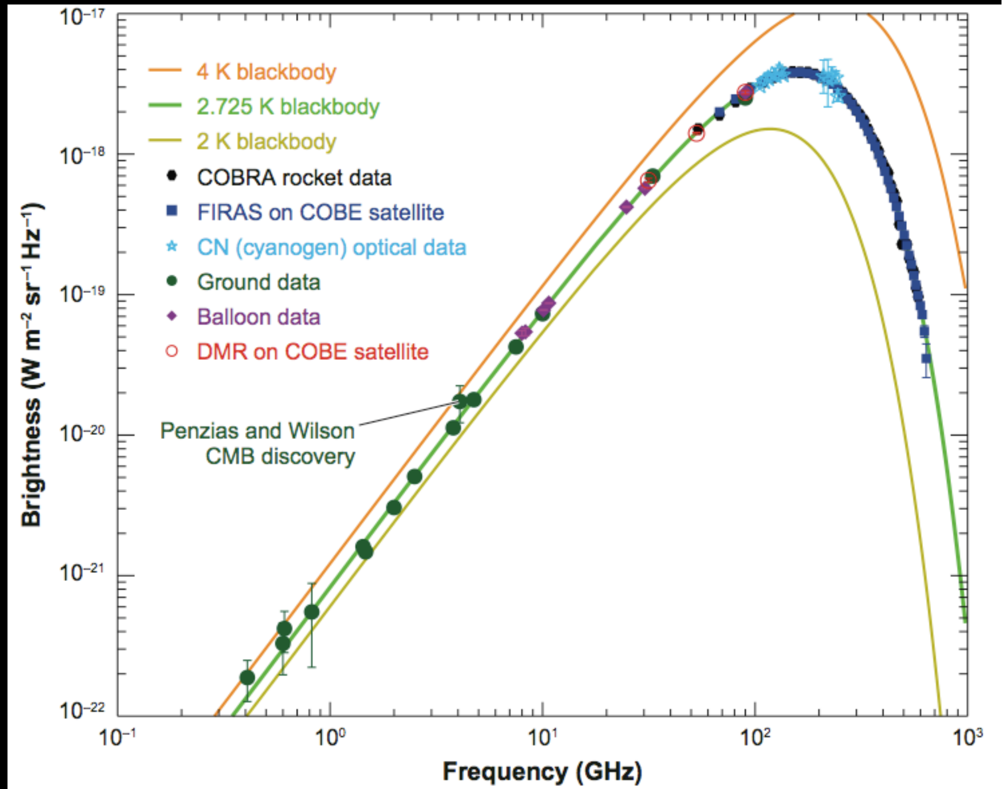

COBE-FIRAS: spectral deviations from a blackbody are very small: $|\mu| < 9$ e-5

Refs: Peebles, Physical Cosmology, Cambridge U.P., 1991; Burigana et al. A&A, 1991, 246, 49

CMB polarization

- Polarization in electromagnetic waves

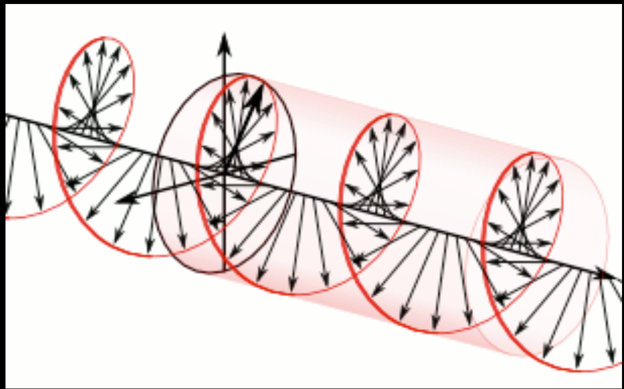

- Polarization is described by the stokes parameters:

$$
\begin{aligned}
I &= |E_x|^2 + |E_y|^2, \\
Q &= |E_x|^2 - |E_y|^2, \\
U &= 2\mathrm{Re}(E_x E_y^*), \\
V &= 2\mathrm{Im}(E_x E_y^*),
\end{aligned}
$$

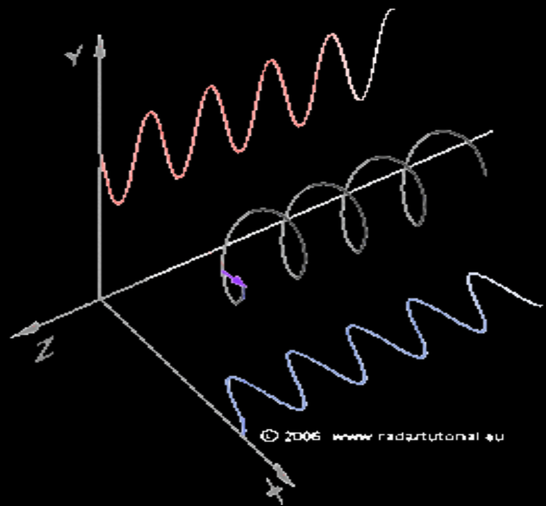

with $Q^2 + U^2 + V^2 = I^2$,

CMB polarization

- The CMB is linearly polarized (quadropole Compton scattering)

- Reference frame independent polarization modes:

  - E-mode polarization:
    - has a vanishing curl (like the Electric field)
    - arises from Thomson scattering in non-homogeneous media
    - it has been measured by WMAP and other CMB experiments

  - B-model polarization:
    - has vanishing divergence (like the Magnetic B field)
    - arises by tensor perturbations (primordial gravitational waves)
    - it has not been measured. It depends on the scalar to tensor ratio. If observed gives most important information about the primordial universe

- CMB E and B mode polarizations can be generated before (primary CMB polarization) and after decoupling (secondary CMB polarization by sources)

CMB polarization

- Conversion between polarization modes: (Q, U) to (E, B)

APPENDIX

ANGULAR POWER SPECTRUM COMPUTATION

Since Q and U depend on the coordinate system, it is more convenient to work with maps of the scalar E and pseudo-scalar B modes, which are reference frame independent quantities. In terms of parity transformation, E remains unchanged but the sign of B changes in analogy with the electric and magnetic fields, respectively (e.g. Zaldarriaga & Seljak 1997; Kamionkowski et al. 1997; Zaldarriaga 1998). Using the relations (9), (10) and the linear combination between $a_{\pm 2,lm}$, E and B can be defined as

$$E(\hat{n}) = \sum_{\ell}\sum_{m} a_{E,\ell m} Y_{\ell m}(\hat{n}) \tag{A1}$$

$$B(\hat{n}) = \sum_{\ell}\sum_{m} a_{B,\ell m} Y_{\ell m}(\hat{n}) \tag{A2}$$

with $a_{E,\ell m}$=-$(a_{2,\ell m}$+$a_{-2,lm})/2$ and $a_{B,\ell m}$=i$(a_{2,\ell m}$-$a_{-2,\ell m})/2$. For small sky patches, Q_T and U_T can be decomposed in the Fourier domain as

$$Q_T(\vec{\theta}) = \frac{1}{(2\pi)^2}\int [E(\vec{\ell})cos(2\alpha) - B(\vec{\ell})sin(2\alpha)]e^{i\vec{\ell}.\vec{\theta}}d^2\vec{\ell} \tag{A3}$$

$$U_T(\vec{\theta}) = \frac{1}{(2\pi)^2}\int [E(\vec{\ell})sin(2\alpha) + B(\vec{\ell})cos(2\alpha)]e^{i\vec{\ell}.\vec{\theta}}d^2\vec{\ell} \tag{A4}$$

where α is the angle between the mode $\vec{\ell}$ and the Fourier plane. The power spectra of the E and B modes can be computed directly in the Fourier space by preforming the Fourier transform (FT) of the previous relations, resulting in

$$E(\vec{\ell}) = \int [\tilde{Q}_T cos(2\alpha) + \tilde{U}_T sin(2\alpha)]e^{-i\vec{\ell}.\vec{\theta}}d^2\vec{\theta} \tag{A5}$$

$$B(\vec{\ell}) = \int [-\tilde{Q}_T sin(2\alpha) + \tilde{U}_T cos(2\alpha)]e^{-i\vec{\ell}.\vec{\theta}}d^2\vec{\theta} \tag{A6}$$

with $\tilde{Q}_T = FT(Q_T(\vec{\theta}))$ and $\tilde{U}_T = FT(U_T(\vec{\theta}))$. Applying Fourier transforms to these equations we obtain maps of the E and B modes in real space.

Sources of CMB anisotropies

CMB temperature map by Planck

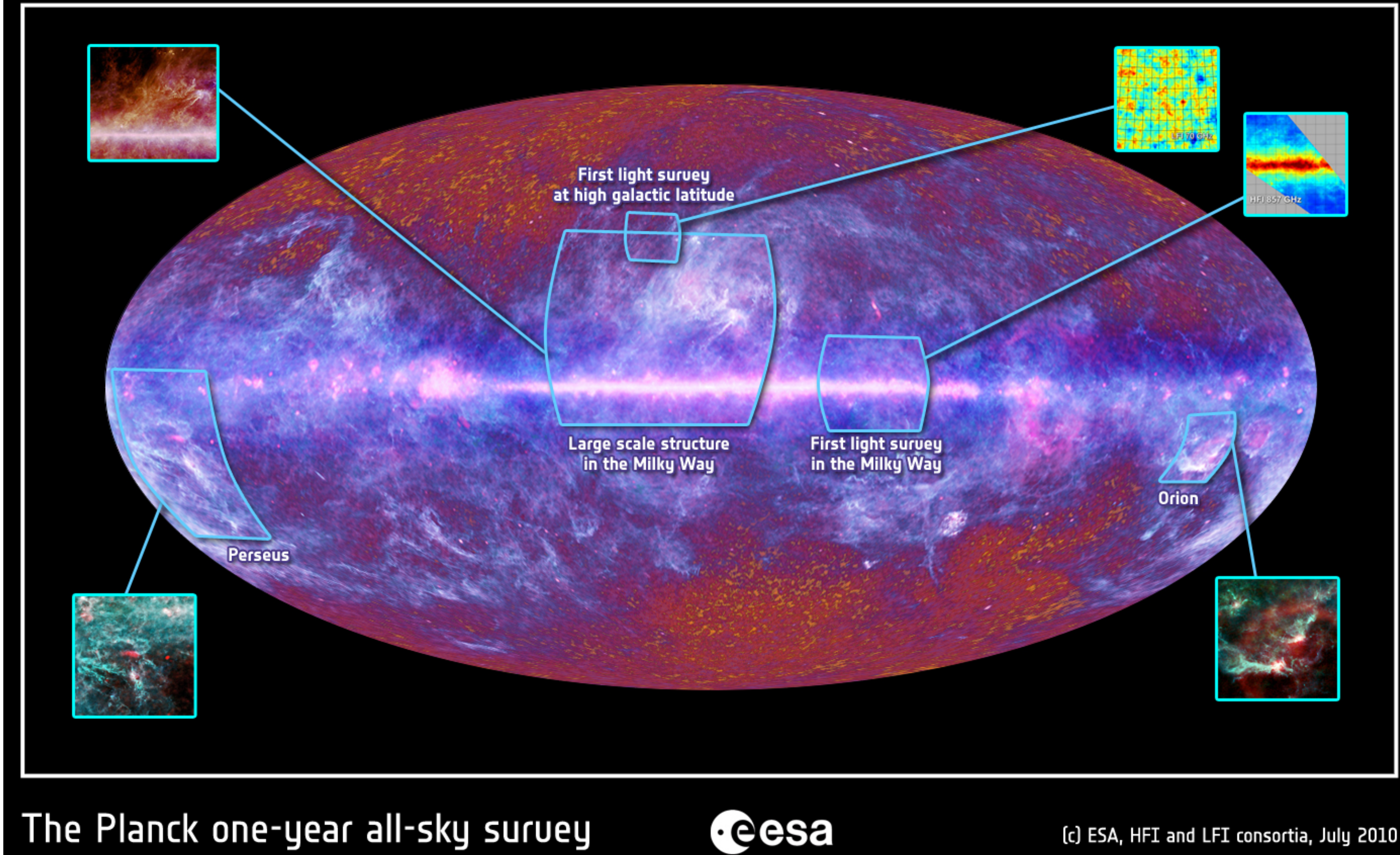

Sources of temperature fluctuations

Primary: intrinsic CMB signal resulting from the properties of the CMB at the Last Scattering Surface (LSS)

• Secondary: CMB signal arising to physical effects acting on the CMB photons during their propagation from the LSS to the observer

• "Terciary": astrophysical foregrounds, solar system, instrumental noise, …

Table 1. Sources of temperature fluctuations.

PRIMARY	Gravity	
	Doppler	
	Density fluctuations	
	Damping	
	Defects	Strings
		Textures
SECONDARY	Gravity	Early ISW
		Late ISW
		Rees-Sciama
		Lensing
	Local reionization	Thermal SZ
		Kinematic SZ
	Global reionization	Suppression
		New Doppler
		Vishniac
"TERTIARY" (foregrounds & headaches)	Extragalactic	Radio point sources
		IR point sources
	Galactic	Dust
		Free-free
		Synchrotron
	Local	Solar system
		Atmosphere
		Noise, *etc.*

Reprinted from: Tegmark, Varena lectures, 1995, astro-ph/9511148

Sources of temperature fluctuations

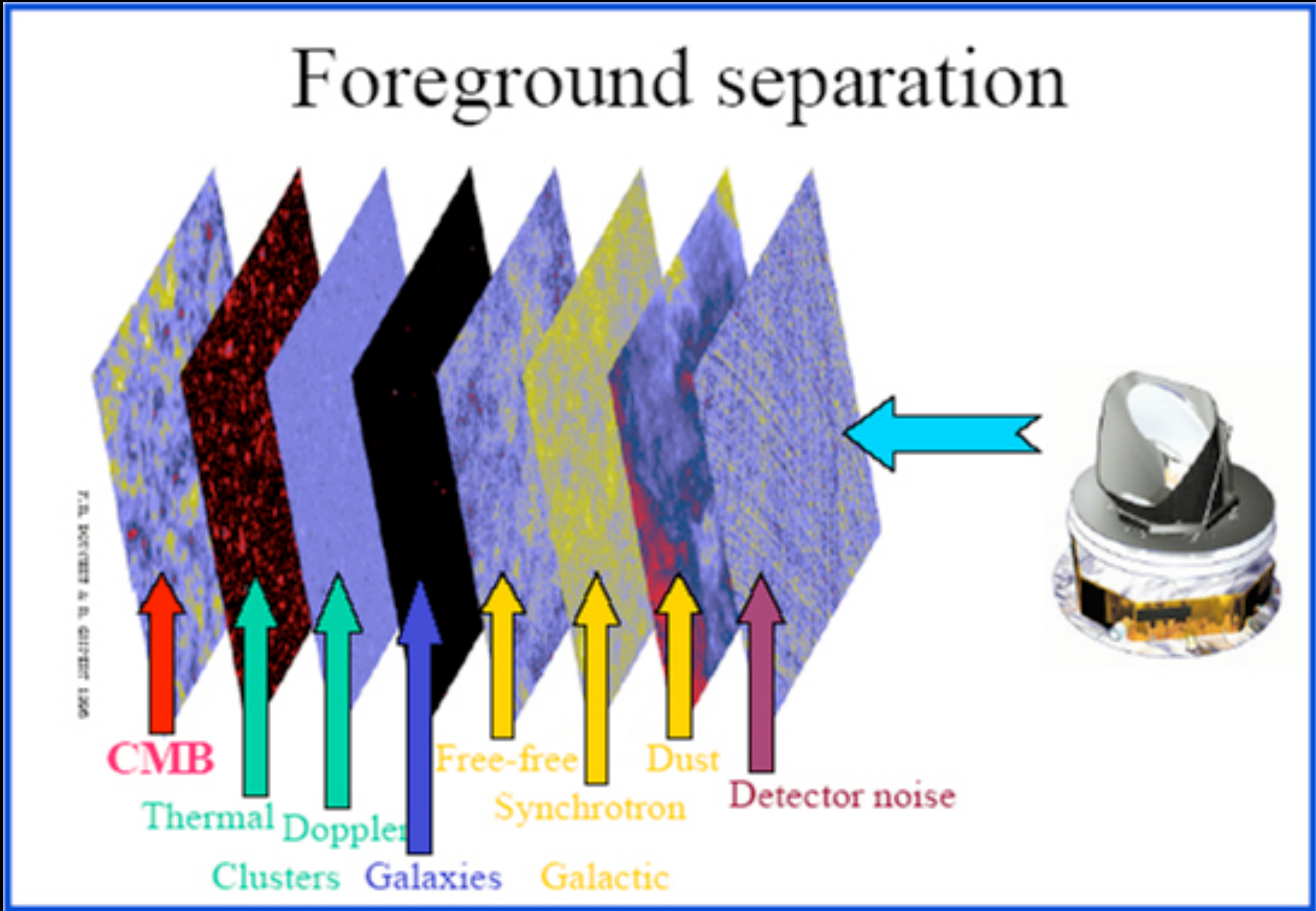

reprinted from: ESA Planck Surveyor red book

Primary anisotropies

$$\frac{\Delta T}{T}(\vec{n}) \approx \phi_e(\vec{n}) + \int_e^o \frac{\partial \phi}{\partial t} dt + \vec{n} \cdot (\vec{v}_o - \vec{v}_e) + \left(\frac{\Delta T}{T}(\vec{n})\right)_e$$

SW	ISW	Doppler	Acoustic Oscillations
(grav.pot @ decoupling)	(grav.pot evolution)	(motion emitters @ dec)	(photon-baryon @ dec)

• Perturbations in the gravitational potential (Sachs-Wolfe effect): photons that last scattered within high-density regions have to climb out of potential wells and are thus redshifted.

• Intrinsic adiabatic perturbations: in high-density regions, the coupling of matter and radiation will also compress the radiation, giving a higher temperature.

• Velocity (Doppler) perturbations: photons last-scattered by matter with a non-zero velocity along the line-of-sight will receive a Doppler shift.

Main sources of Secondary anisitropies

• Integrated Sachs-Wolfe ISW: arises due to changes of the linear gravitational potential with time, during the propagation of the CMB radiation after decoupling

$$\frac{\Delta T}{T} = \int \dot{\phi}\,[(\hat{r}(\eta), \eta]\; d\eta$$

$$\dot{\phi} = \partial\phi/\partial\eta$$

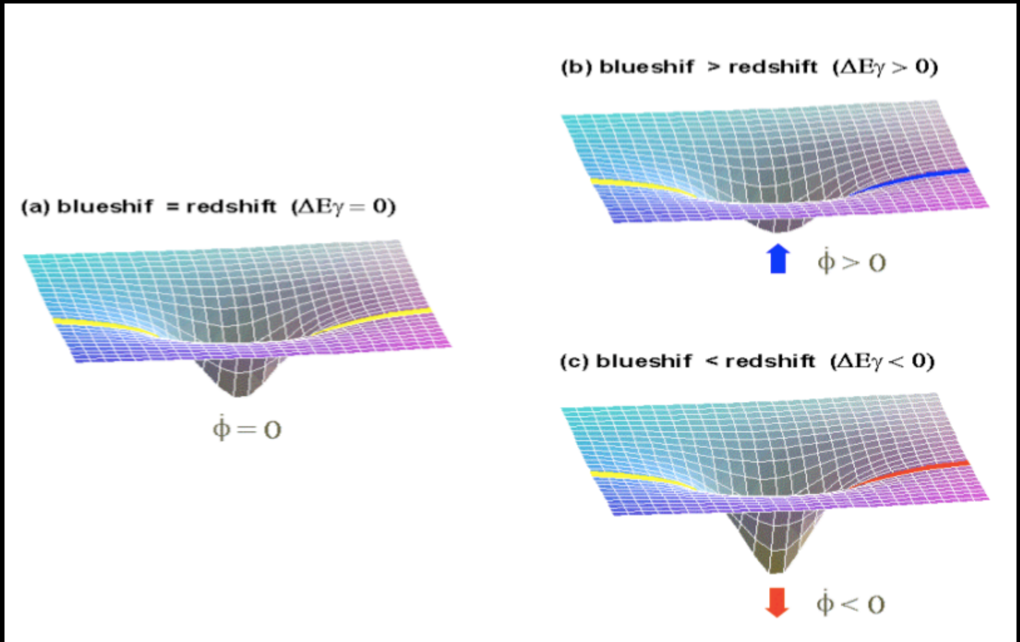

• Early ISW: Relacionado com variações de Φ pouco apos o decoupling (devido a contribuições não desprezaveis da componente de radiação).

• Late ISW: Relacionado com variações de Φ devidas à transição de dominio da Energy Escura

Main sources of Secondary anisitropies

• Rees-Sciama effect: arises due to changes of *non-linear* gravitational potential with time, during the propagation of the CMB radiation after decoupling

$$\frac{\Delta T}{T} = \int \dot{\phi}\left[(\hat{r}(\eta), \eta\right]\, d\eta$$

$$\dot{\phi} = \partial\phi/\partial\eta$$

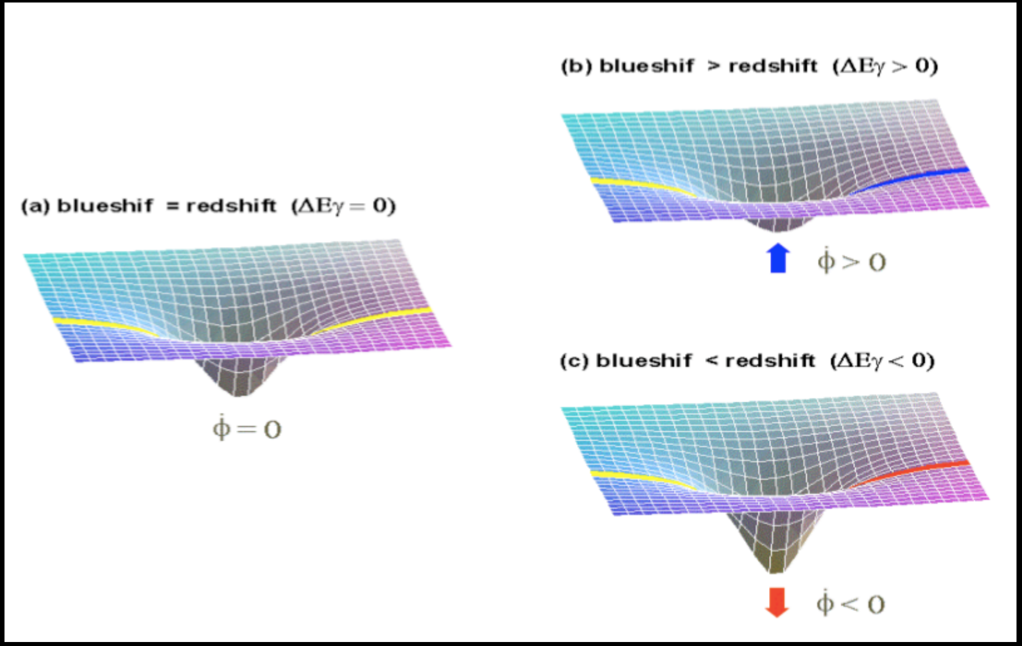

• gravitational lensing of the CMB: the CMB photons are deflected by gravitational lenses, causing redistribution of power on the angular power spectrum. It is stronger at smaller scales, particularly for polarization. I can cause B-mode polarization (from lensed E-mode) primary signal)

Main sources of Secondary anisitropies

• Thermal Sunyaev-Zeldovich effect: arises due to local re-ionization, usualy in galaxy-clusters and super galaxy clusters. The CMB photons suffer inverse Compton scattering (gaining energy) from a thermal population of ionised gas in the clusters. The scattered intensity spectrum in the direction of clusters is no-longer pure Planckian.

• Kinetic Sunyaev-Zeldovich effect: if the clusters have a peculiar velocity along the line of sight, there's an additional Doppler shift proportional to the electron gas cloud.

• Ostriker-Vishniac effect: Associated with global reionization of the Universe. Is the *linear* version of the kinetic Sunyaev-Zeldovich effect. It can strongly suppress CMB anisotropies and generate new ones

Sky statistics: The angular power spectrum

Temperature fluctuation field

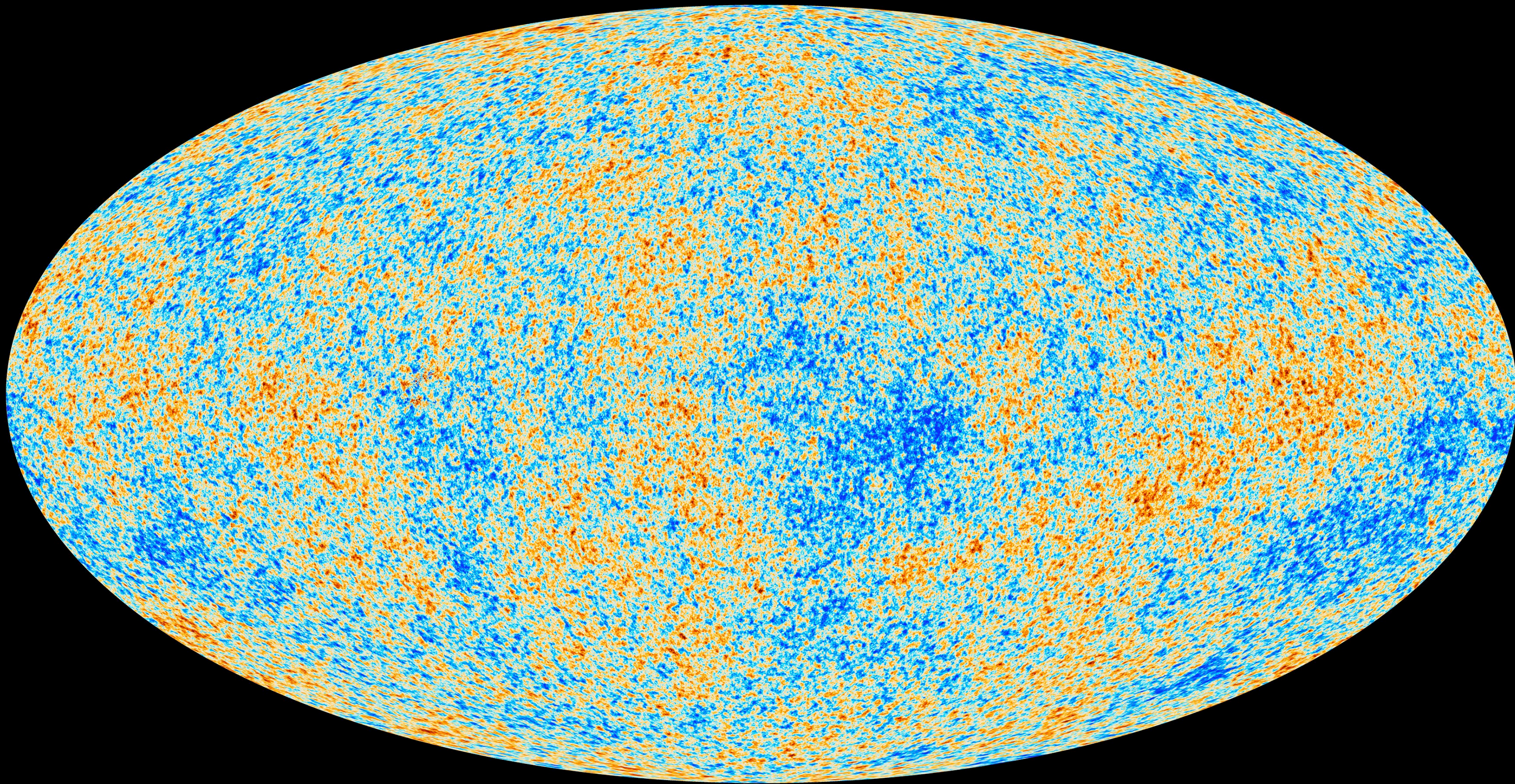

Why a ellipse-like map?

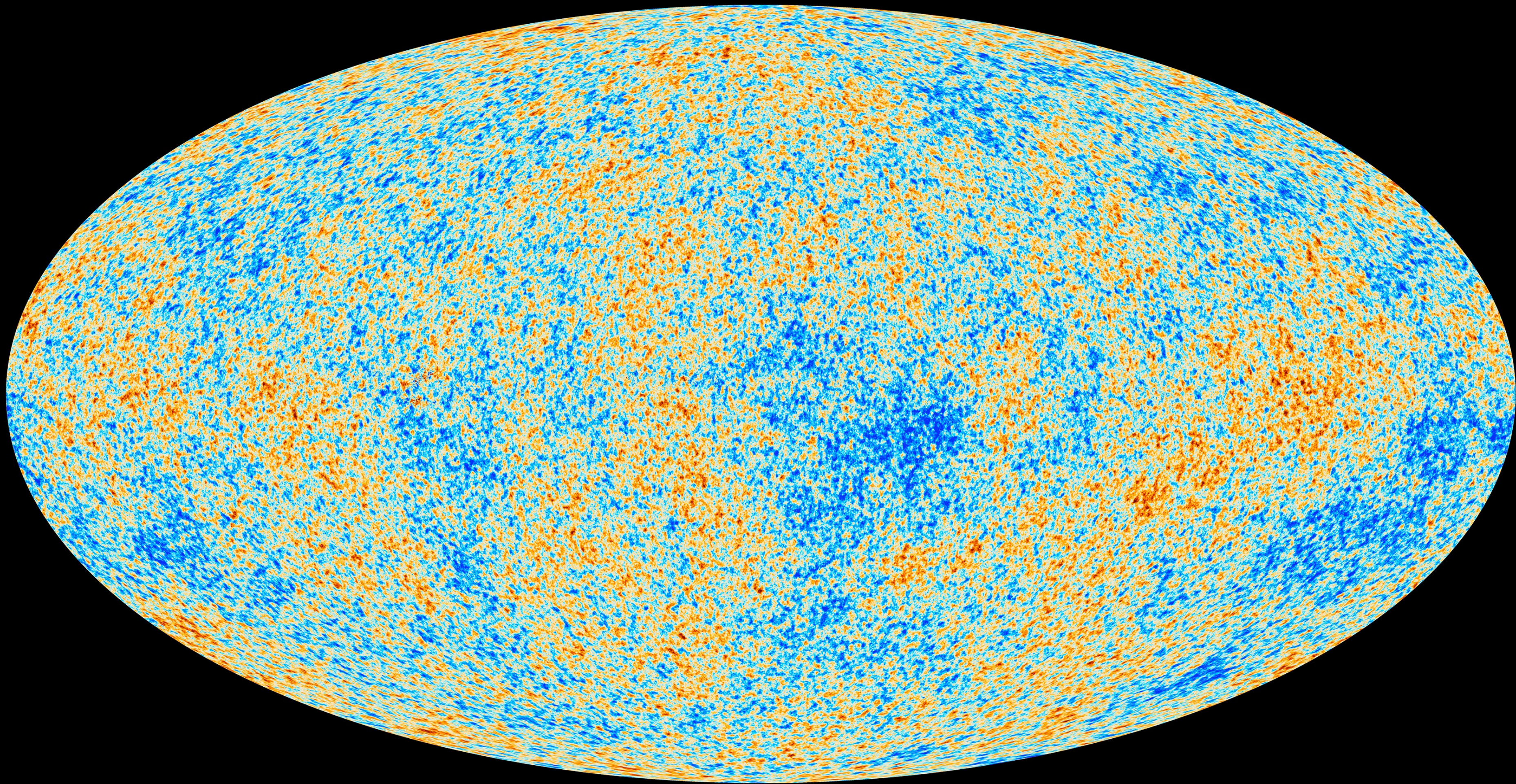

Why a ellipse-like map?

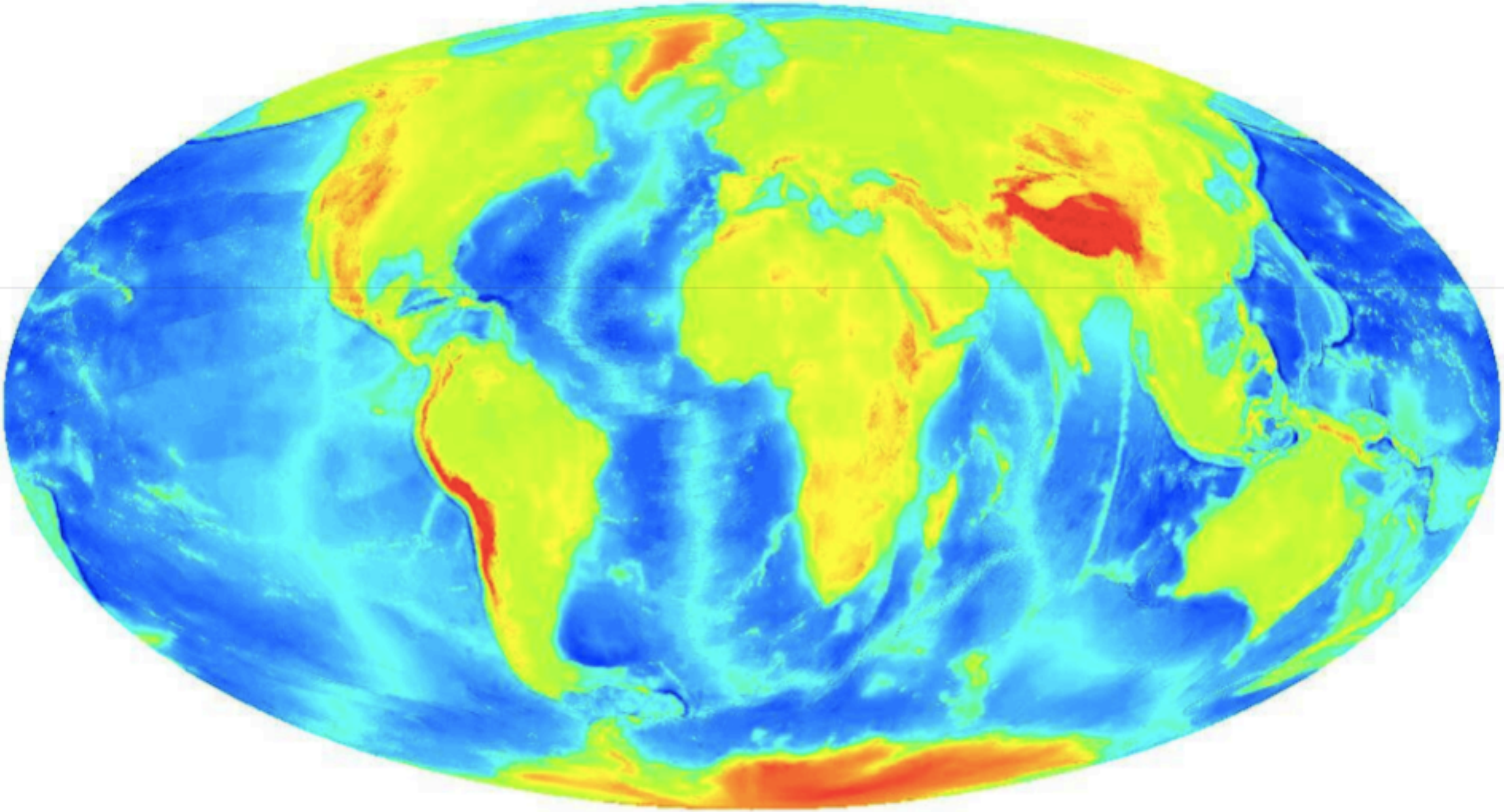

Temperature fluctuation field

- Decomposition of the temperature field on the sky:

$$\Theta(\hat{n}) = \Delta T/T(\theta, \phi) = \sum_{\ell=0}^{\infty} \sum_{m=-\ell}^{\ell} a_{\ell m} Y_{\ell m}(\theta, \phi)$$

- the a_{lm}, the decomposition coeficients, are called multi-pole moments:

$$a_{\ell m} = \int Y^*_{\ell m}(\theta', \phi') \frac{\Delta T}{T}(\theta', \phi') d\Omega'$$

these can be computed directly from the sky map. Are generaly complex quantities.

Spherical harmonics

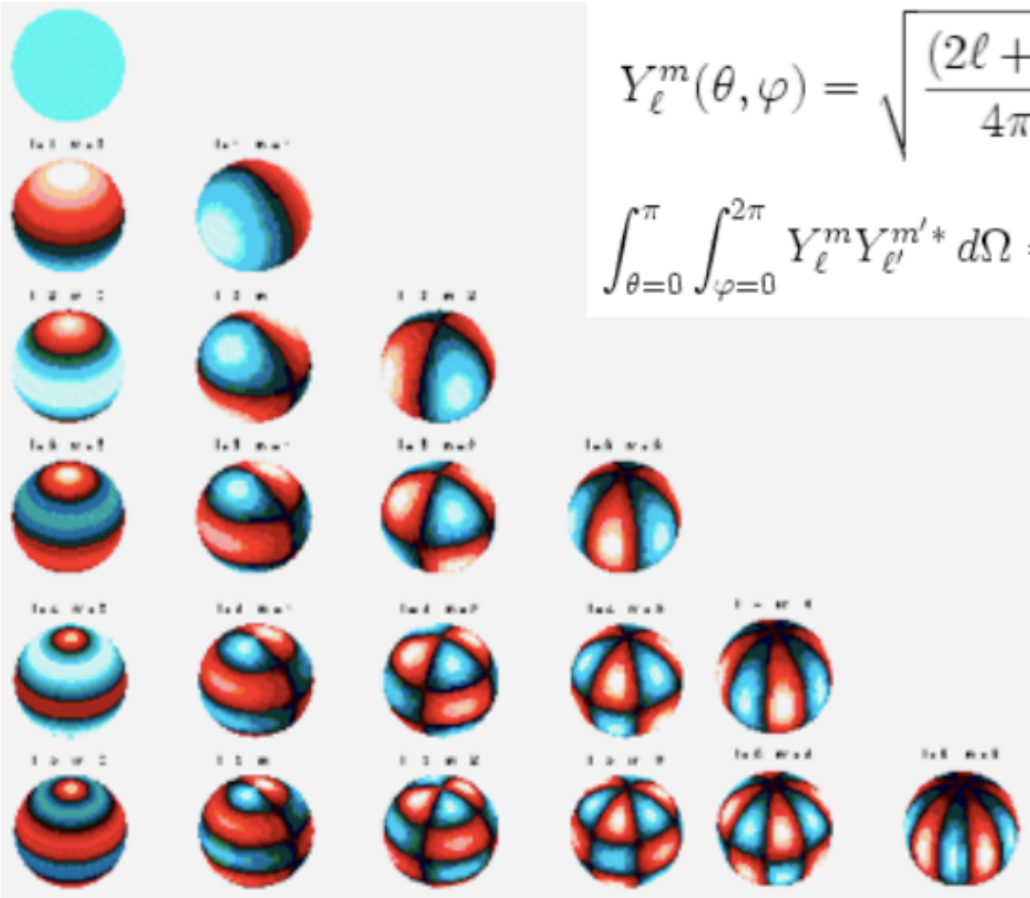

$$Y_\ell^m(\theta,\varphi) = \sqrt{\frac{(2\ell+1)}{4\pi}\frac{(\ell-m)!}{(\ell+m)!}} \cdot e^{im\varphi} \cdot P_\ell^m(\cos\theta)$$

$$\int_{\theta=0}^{\pi}\int_{\varphi=0}^{2\pi} Y_\ell^m Y_{\ell'}^{m'*}\, d\Omega = \delta_{\ell\ell'}\delta_{mm'} \qquad d\Omega = \sin\theta\, d\varphi\, d\theta$$

Spherical harmonics:

Form a vector basis on the sphere

$\ell=1$

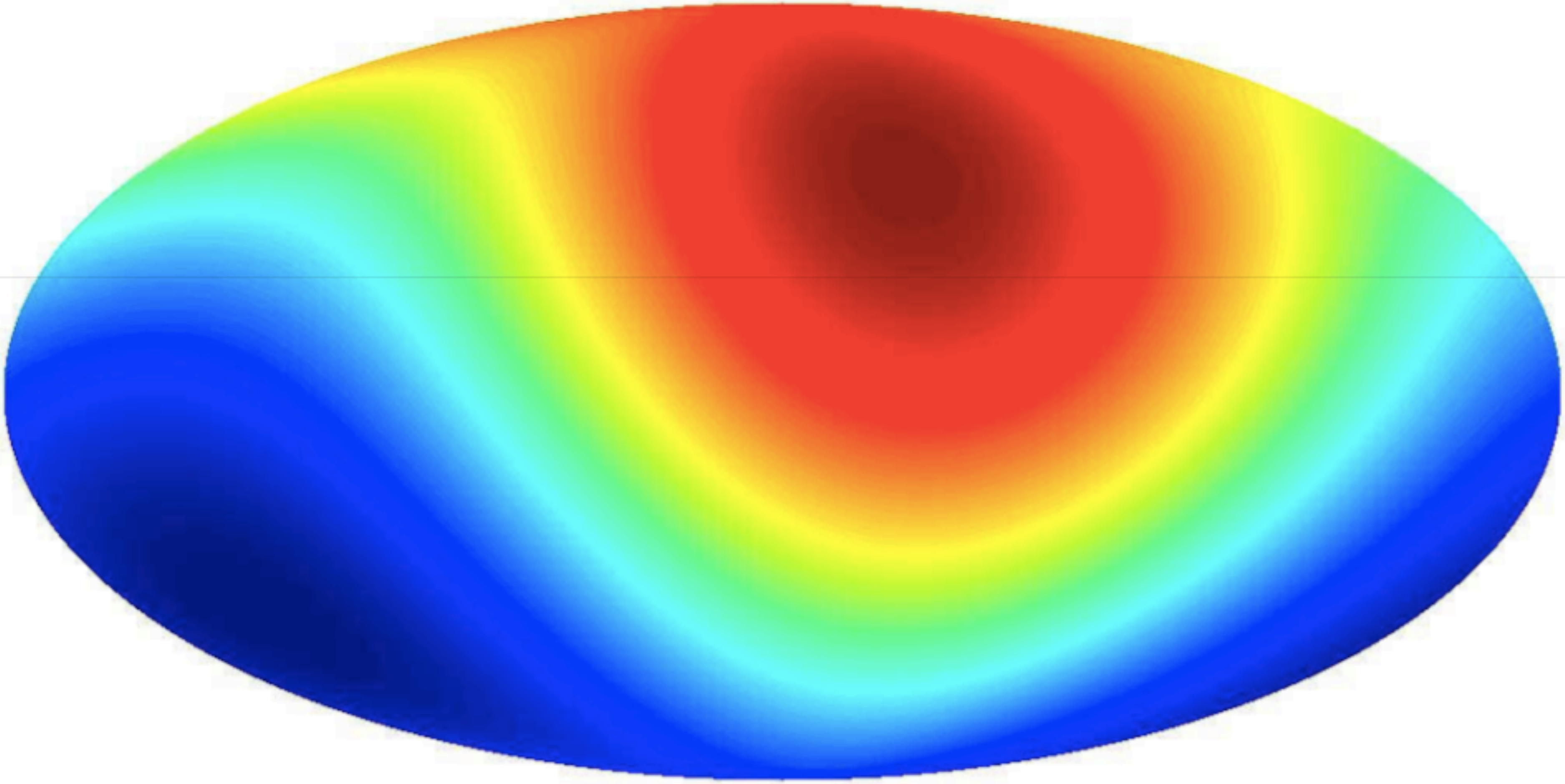

Made by Matthias Bartelmann

ℓ=2

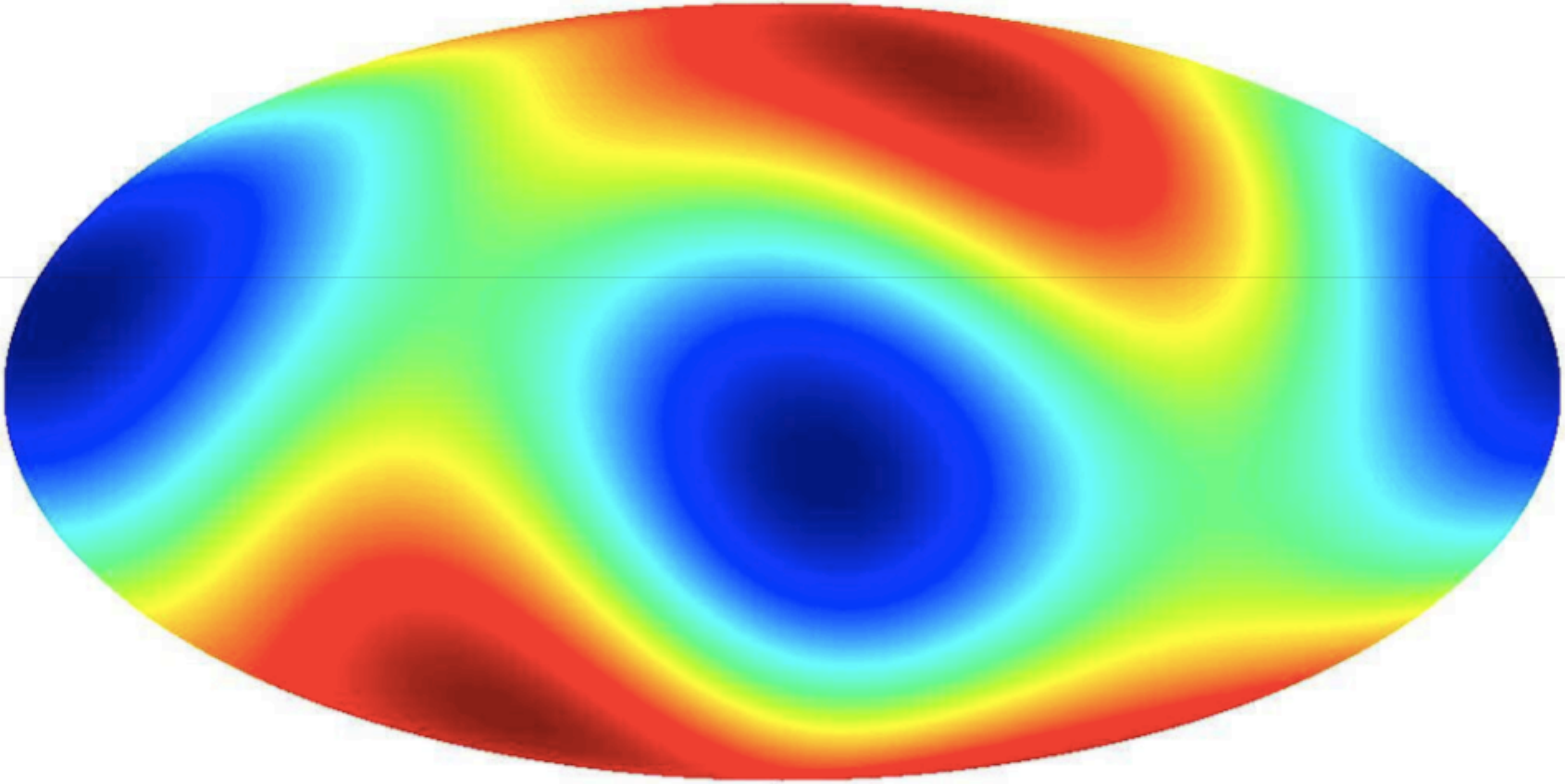

Made by Matthias Bartelmann

ℓ=3

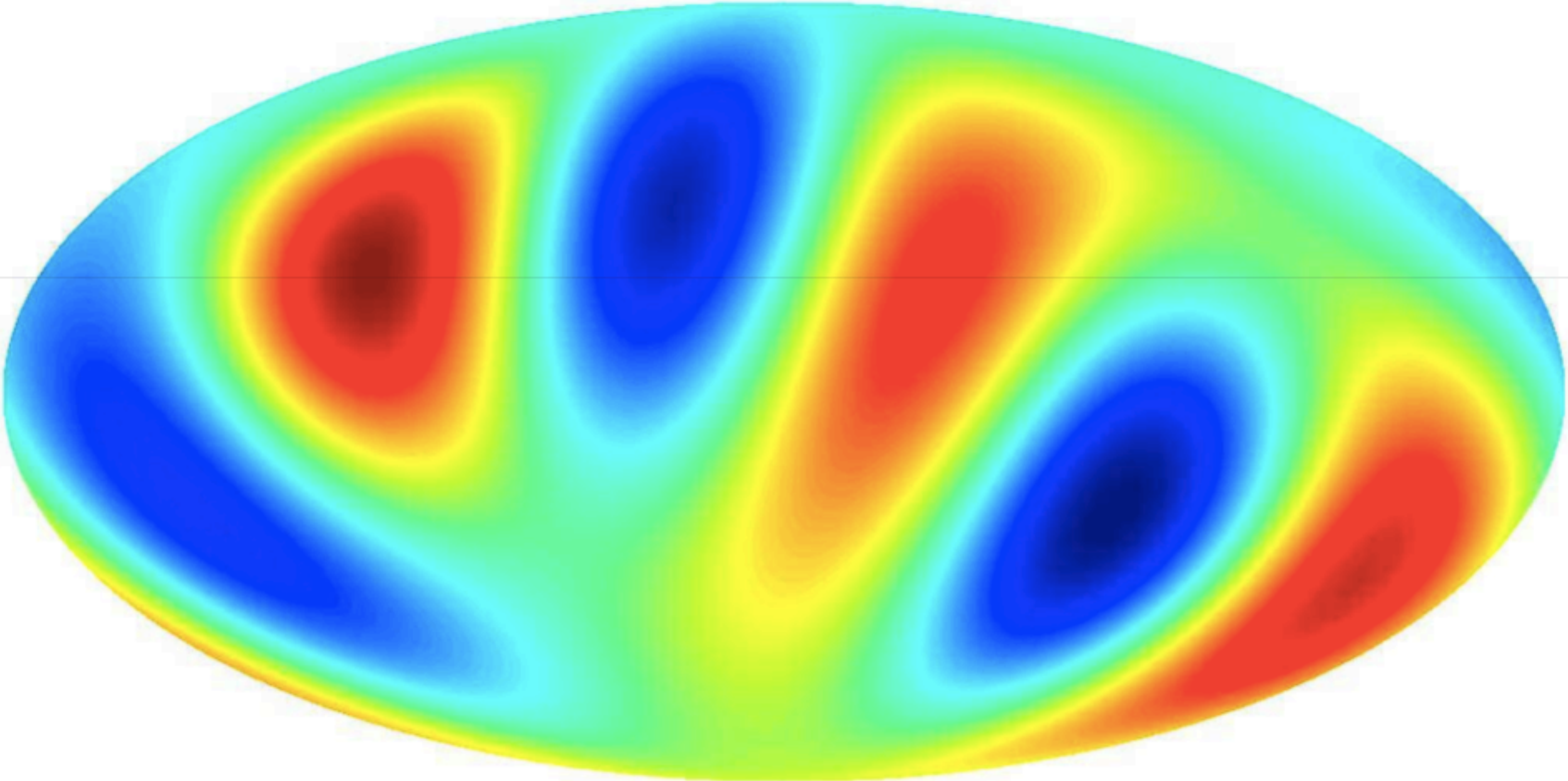

Made by Matthias Bartelmann

$\ell=4$

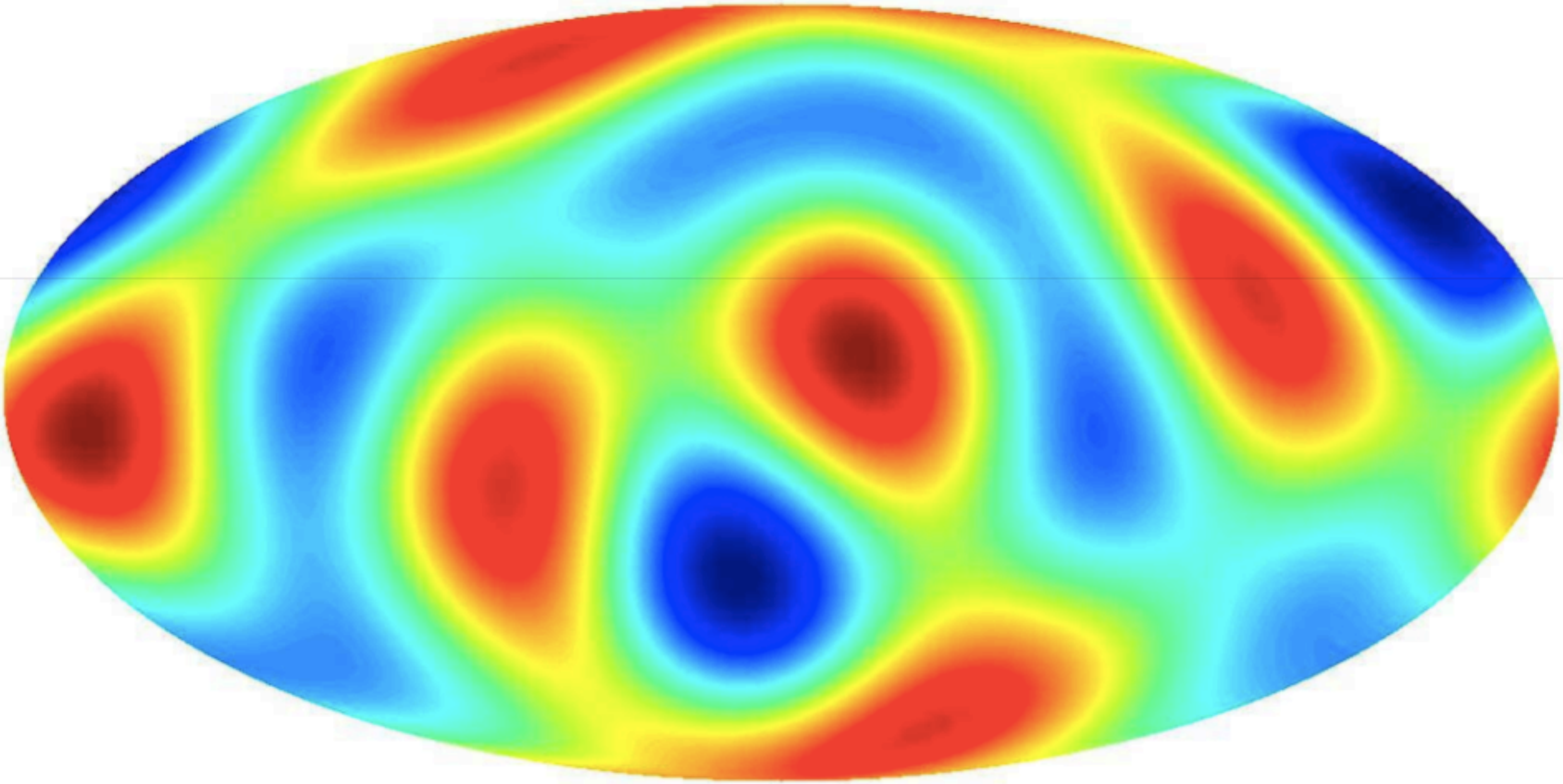

Made by Matthias Bartelmann

ℓ=5

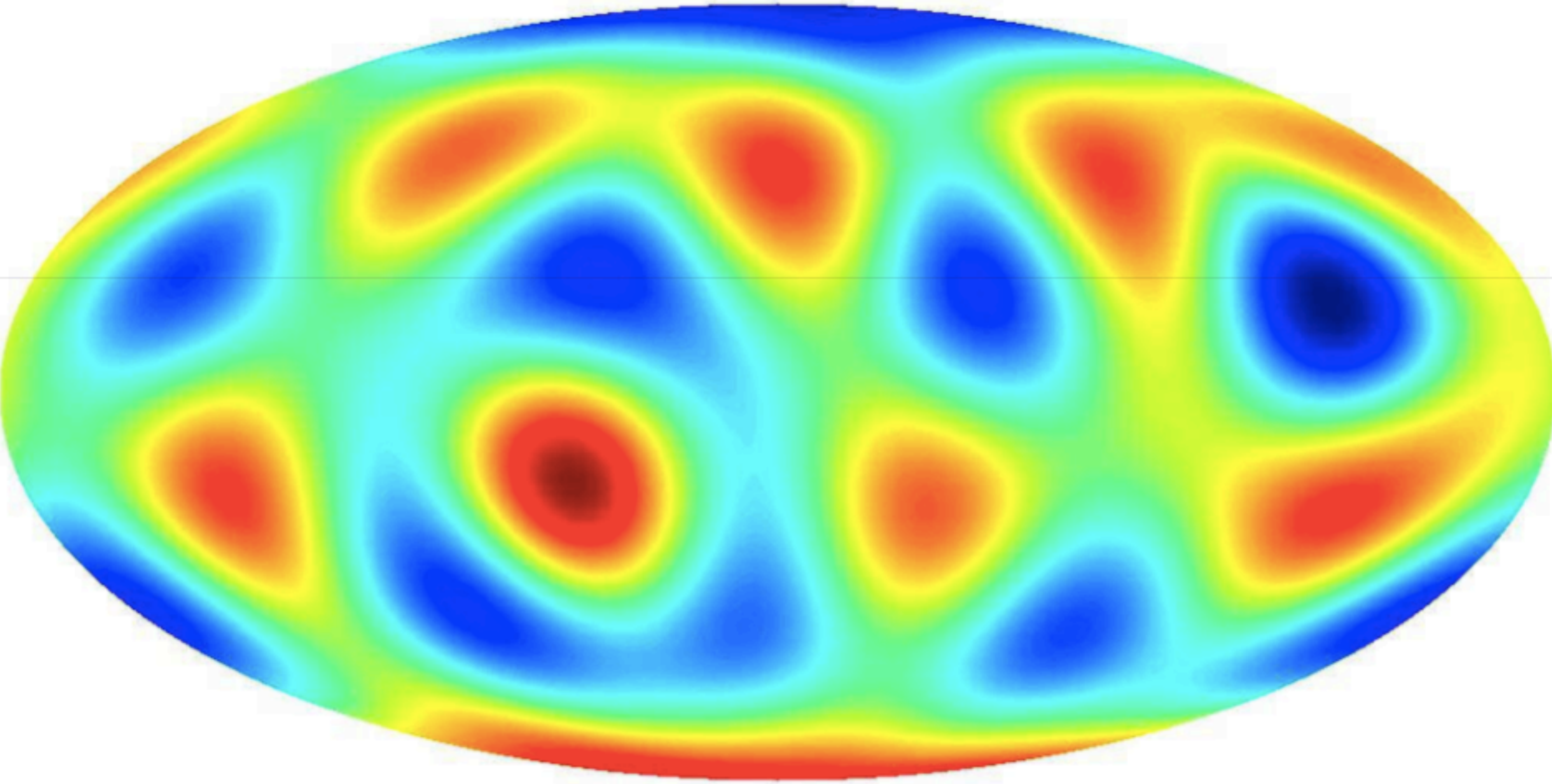

Made by Matthias Bartelmann

ℓ=6

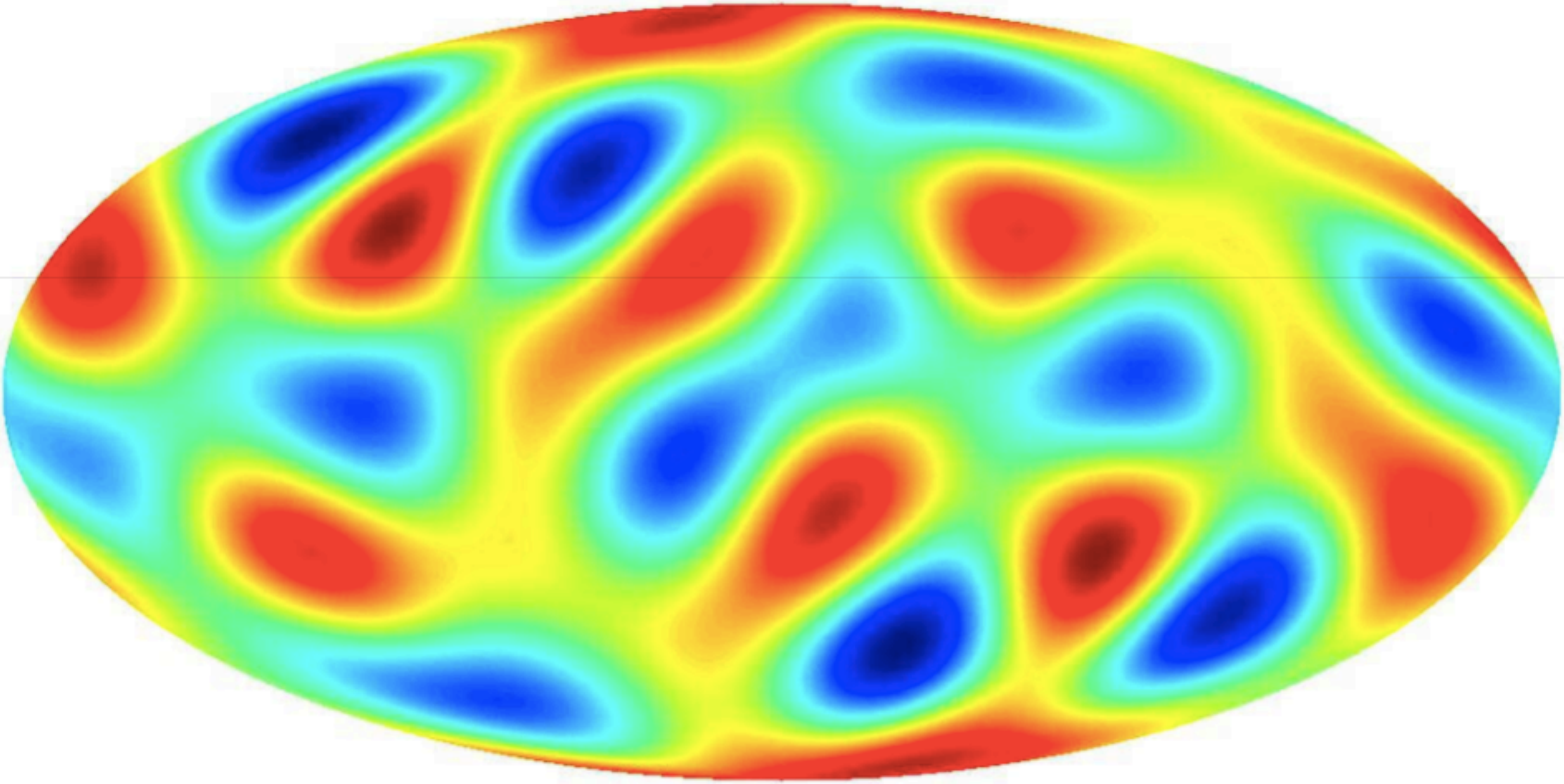

Made by Matthias Bartelmann

$\ell=7$

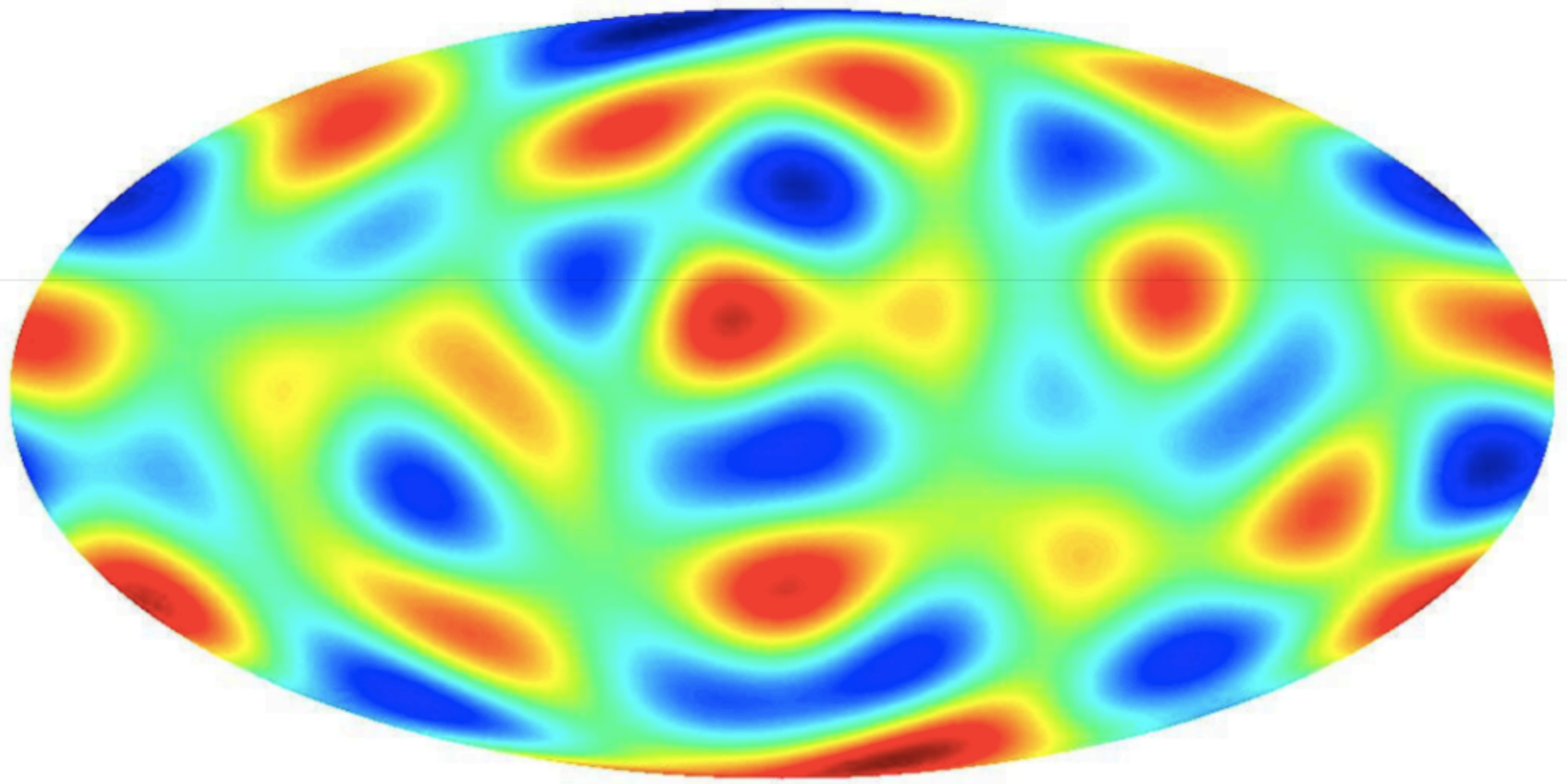

Made by Matthias Bartelmann

ℓ=8

i.e. larger ℓ means shorter wavelengths

i.e. ℓ is spherical equivalent of wavenumber

ℓ ~ pi / theta

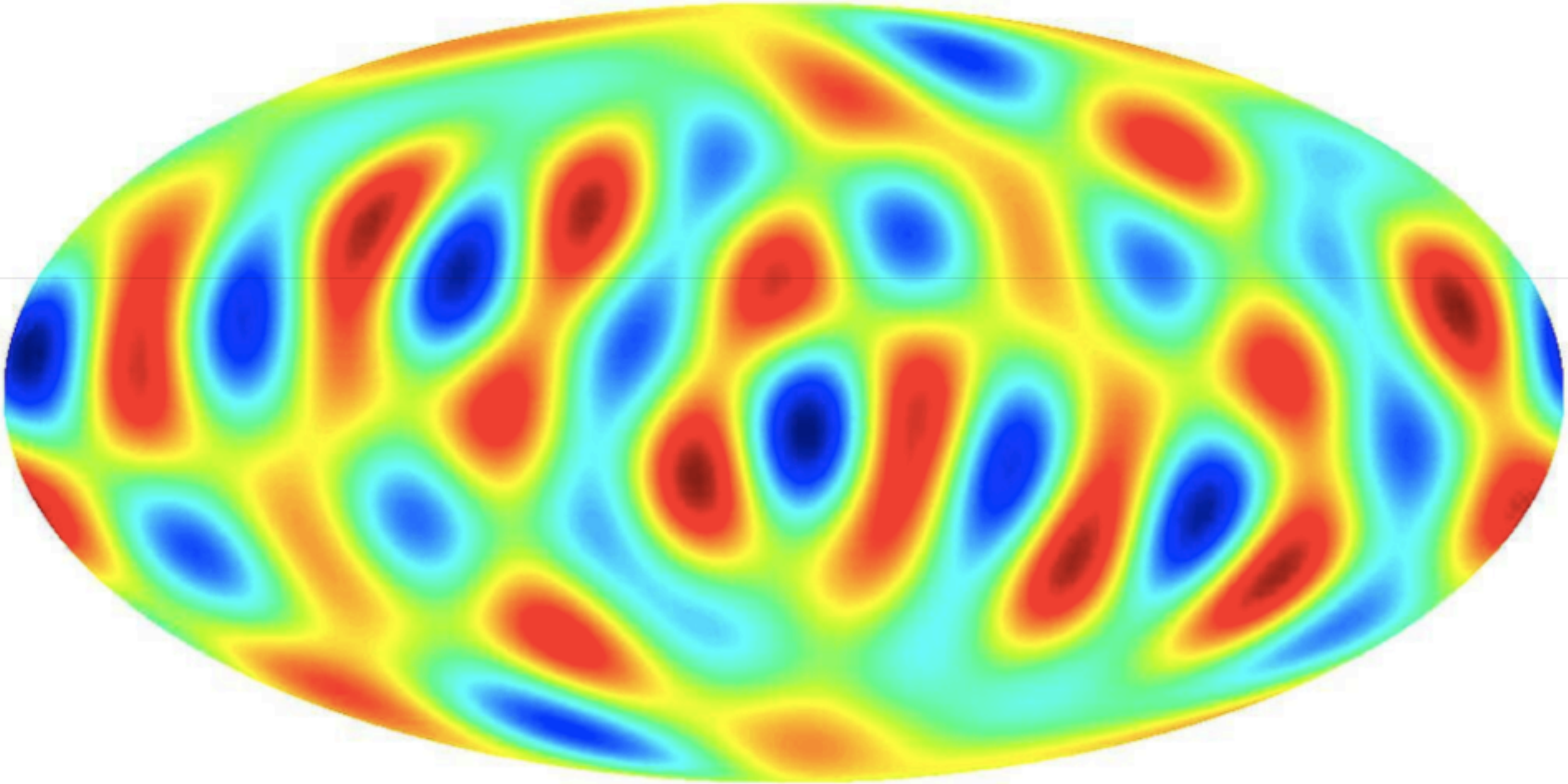

Made by Matthias Bartelmann

$\ell=1$

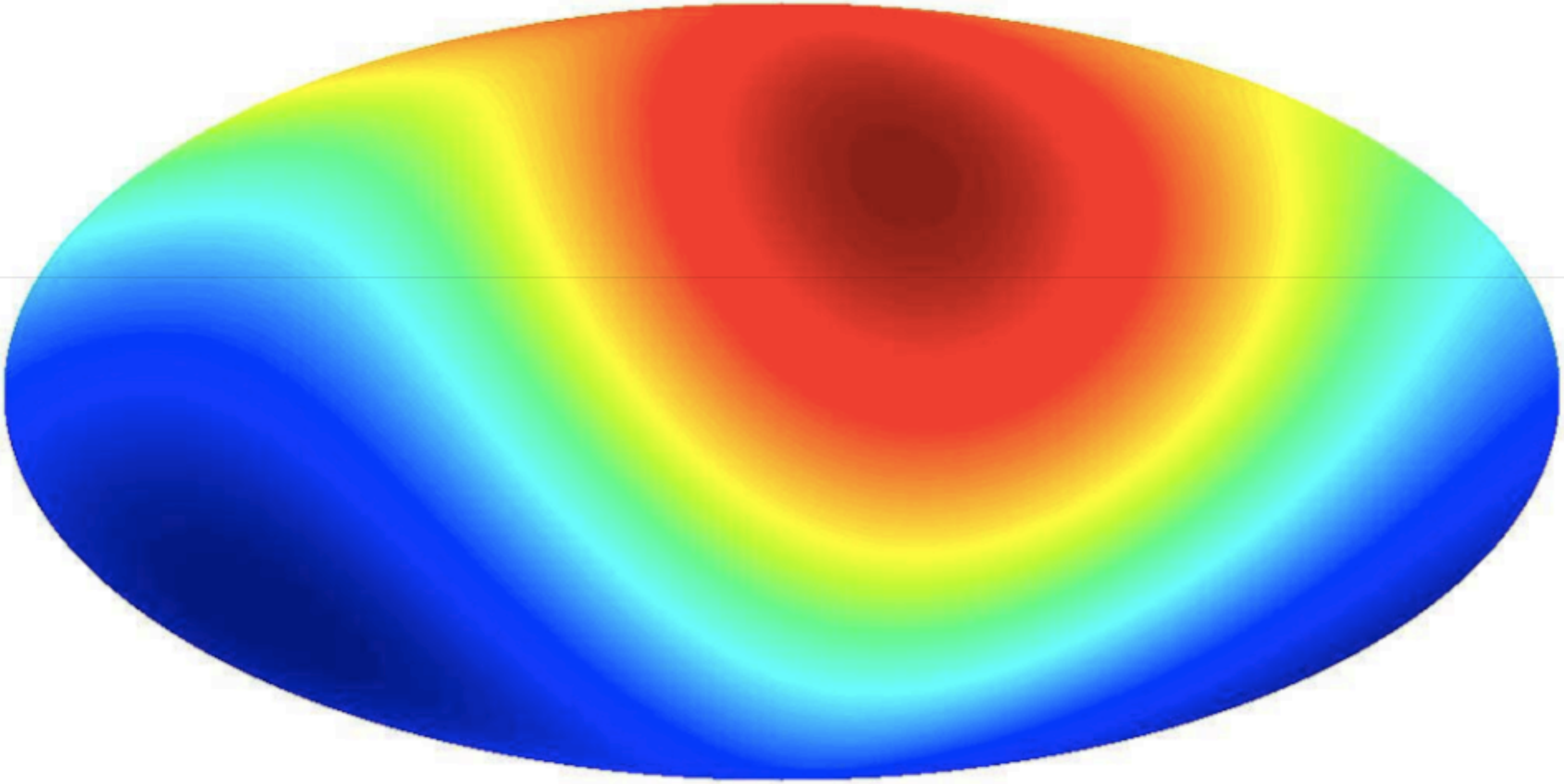

Made by Matthias Bartelmann

ℓ=1 plus ℓ=2

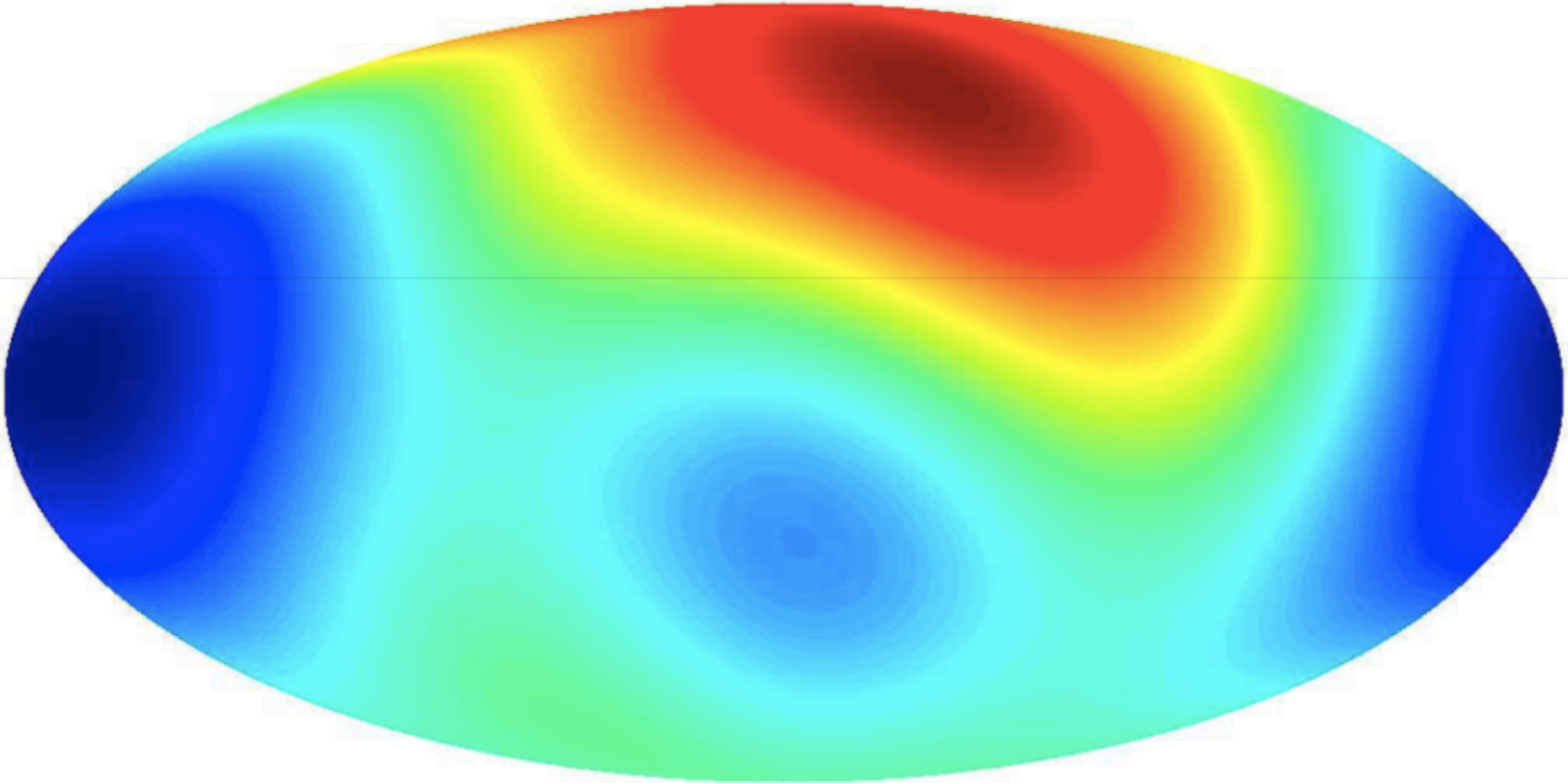

Made by Matthias Bartelmann

ℓ=1 plus ℓ=2 plus ℓ=3

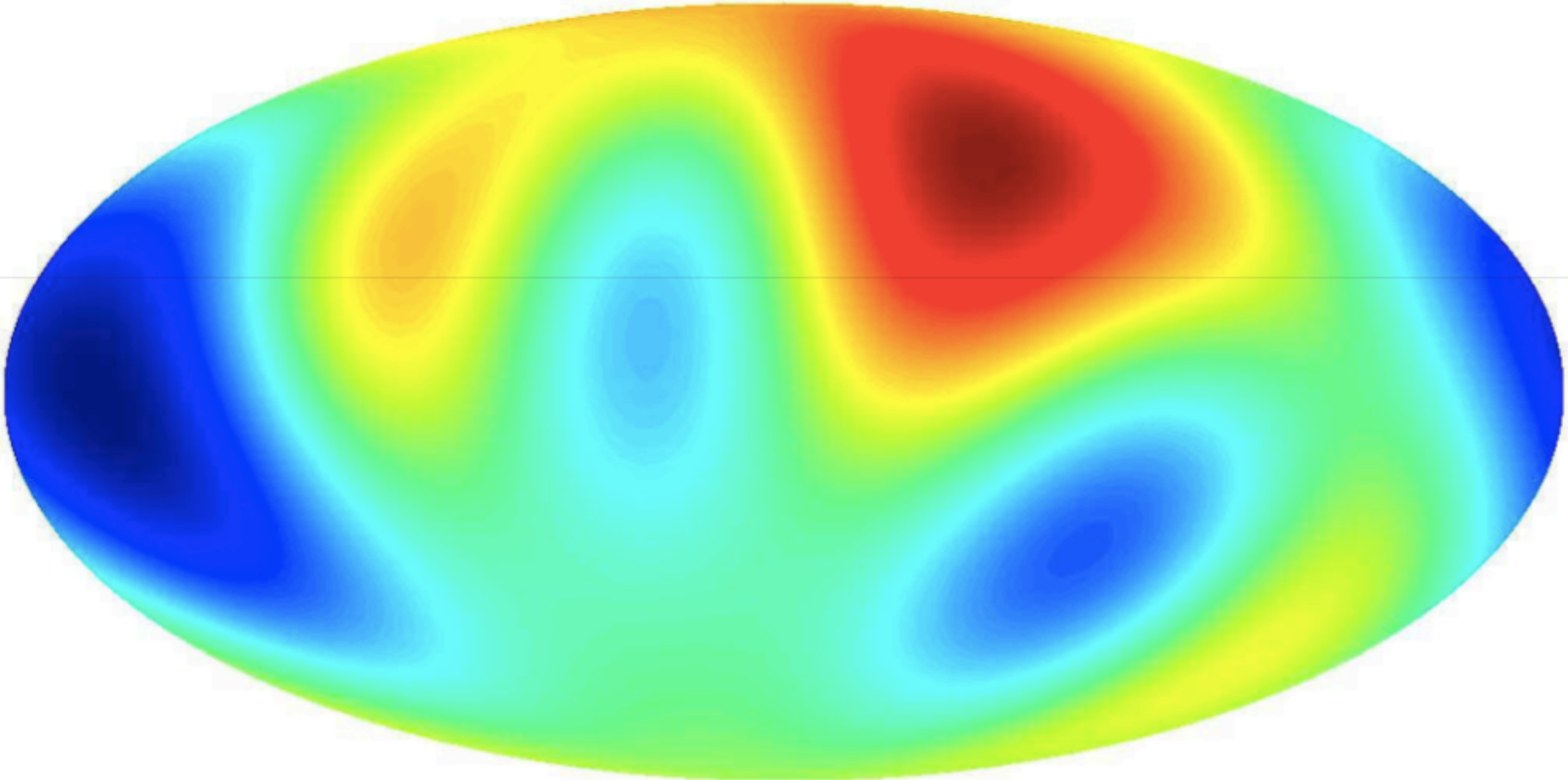

Made by Matthias Bartelmann

Sum ℓ=1 to 4

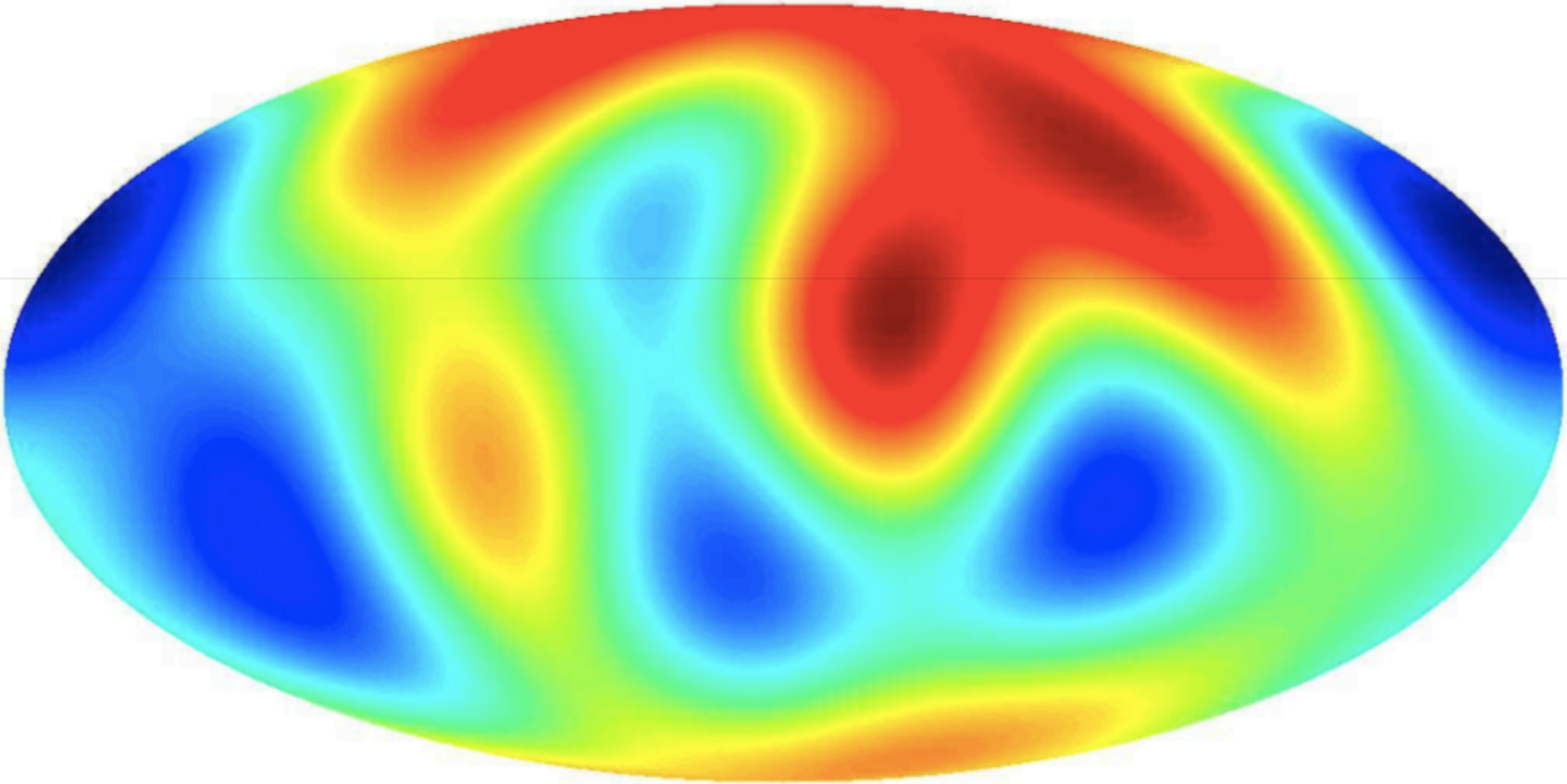

Made by Matthias Bartelmann

Sum ℓ=1 to 5

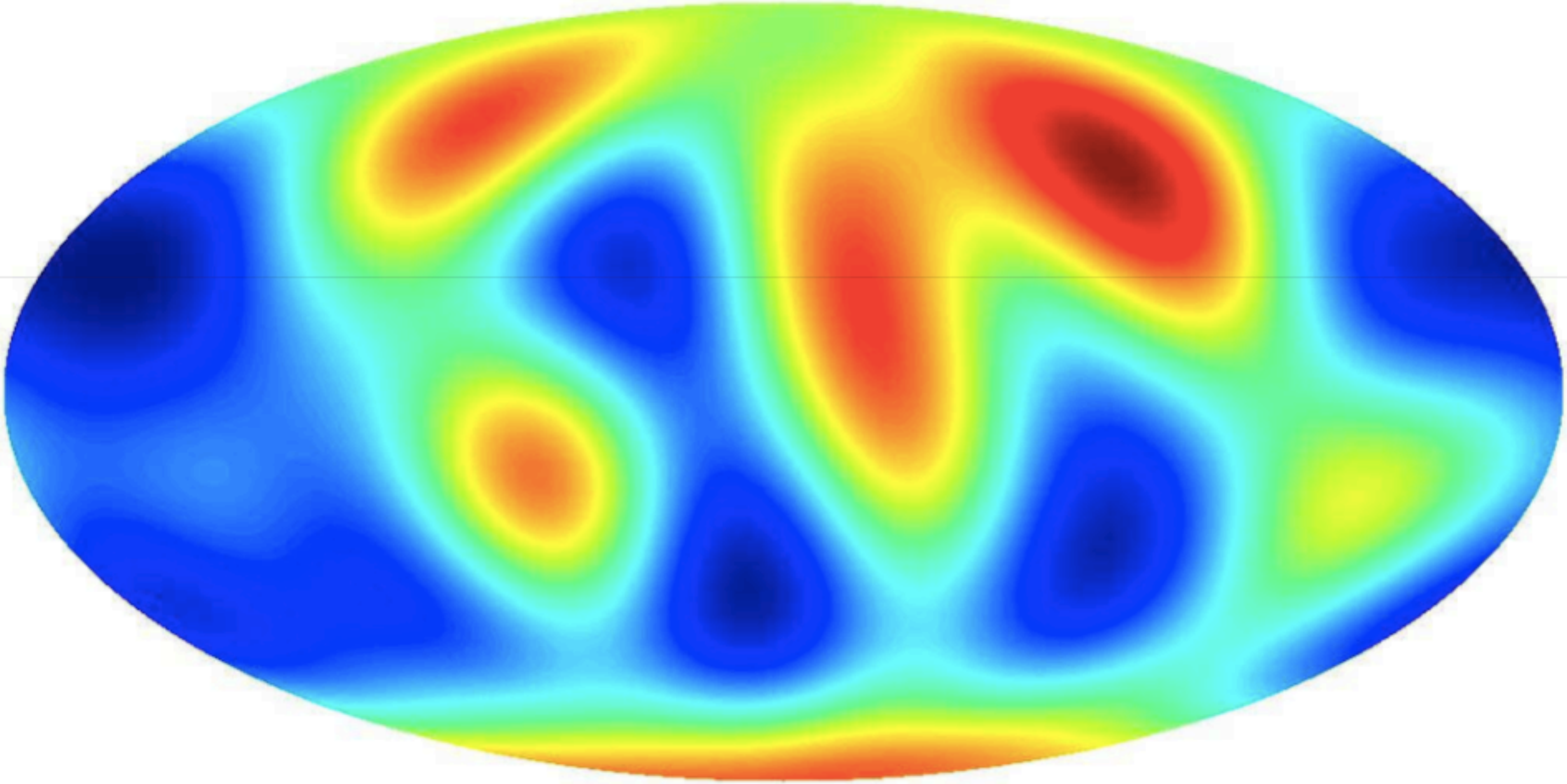

Made by Matthias Bartelmann

Sum ℓ=1 to 6

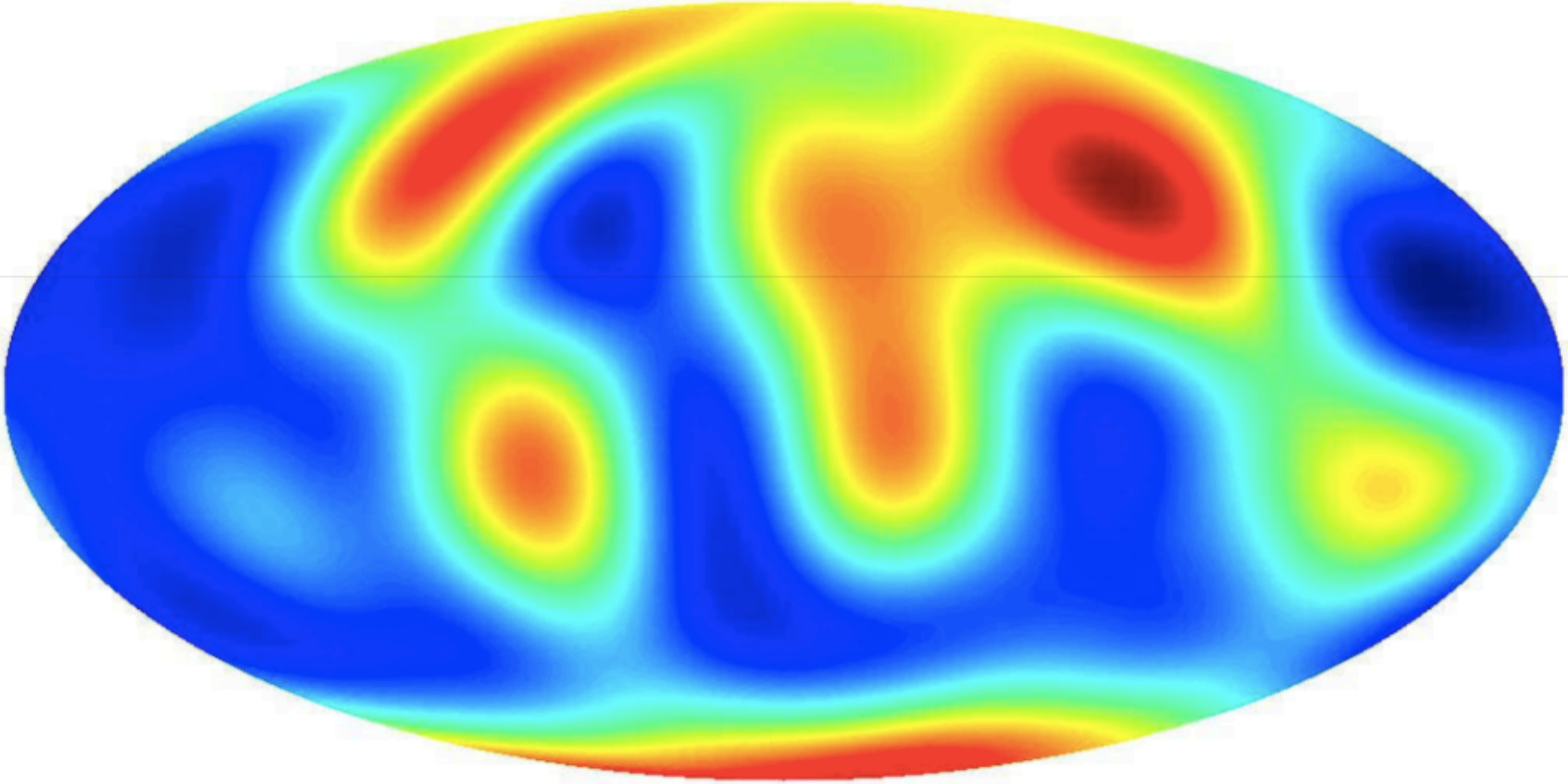

Made by Matthias Bartelmann

Sum ℓ=1 to 7

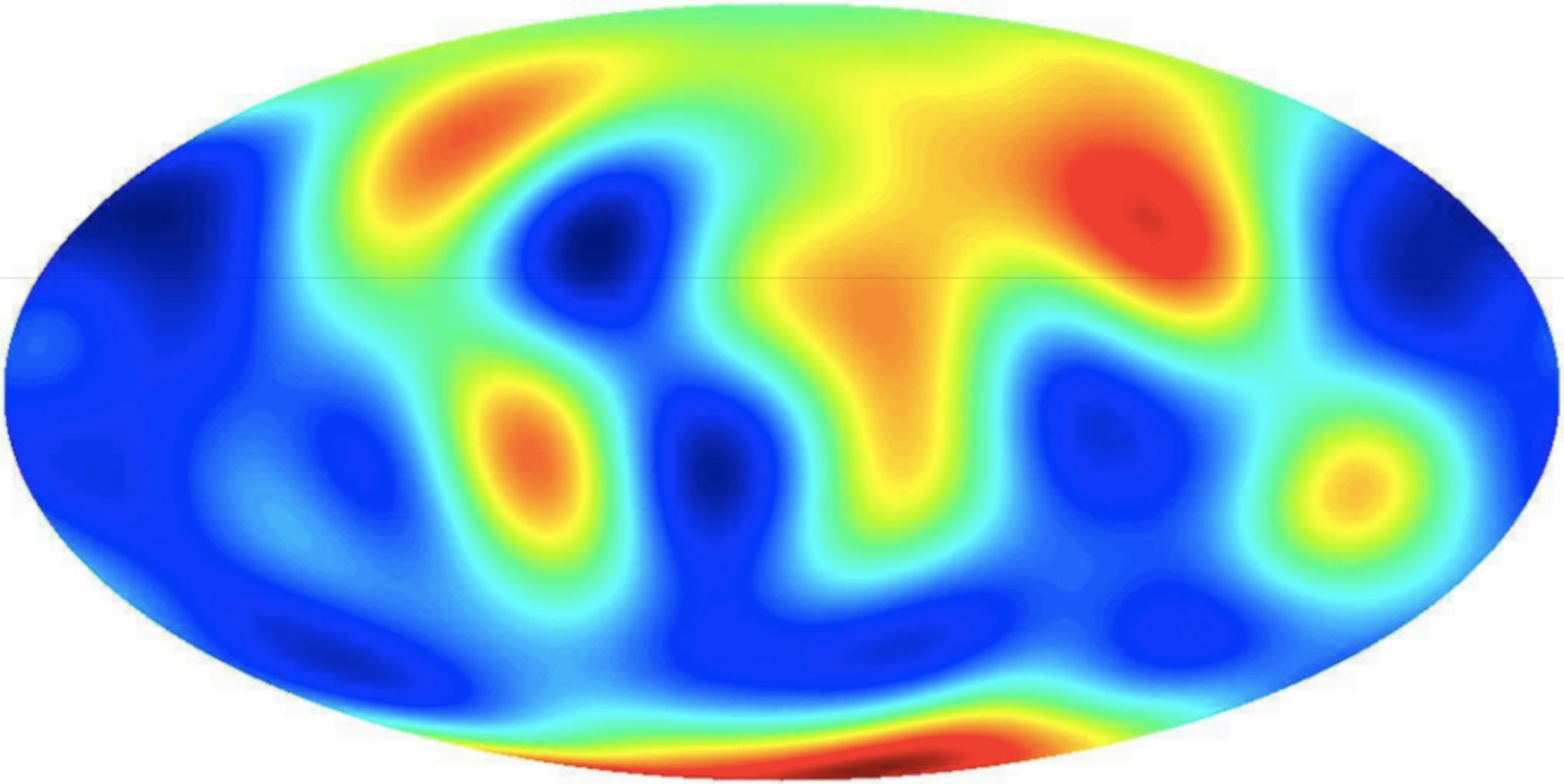

Made by Matthias Bartelmann

Sum ℓ=1 to 8

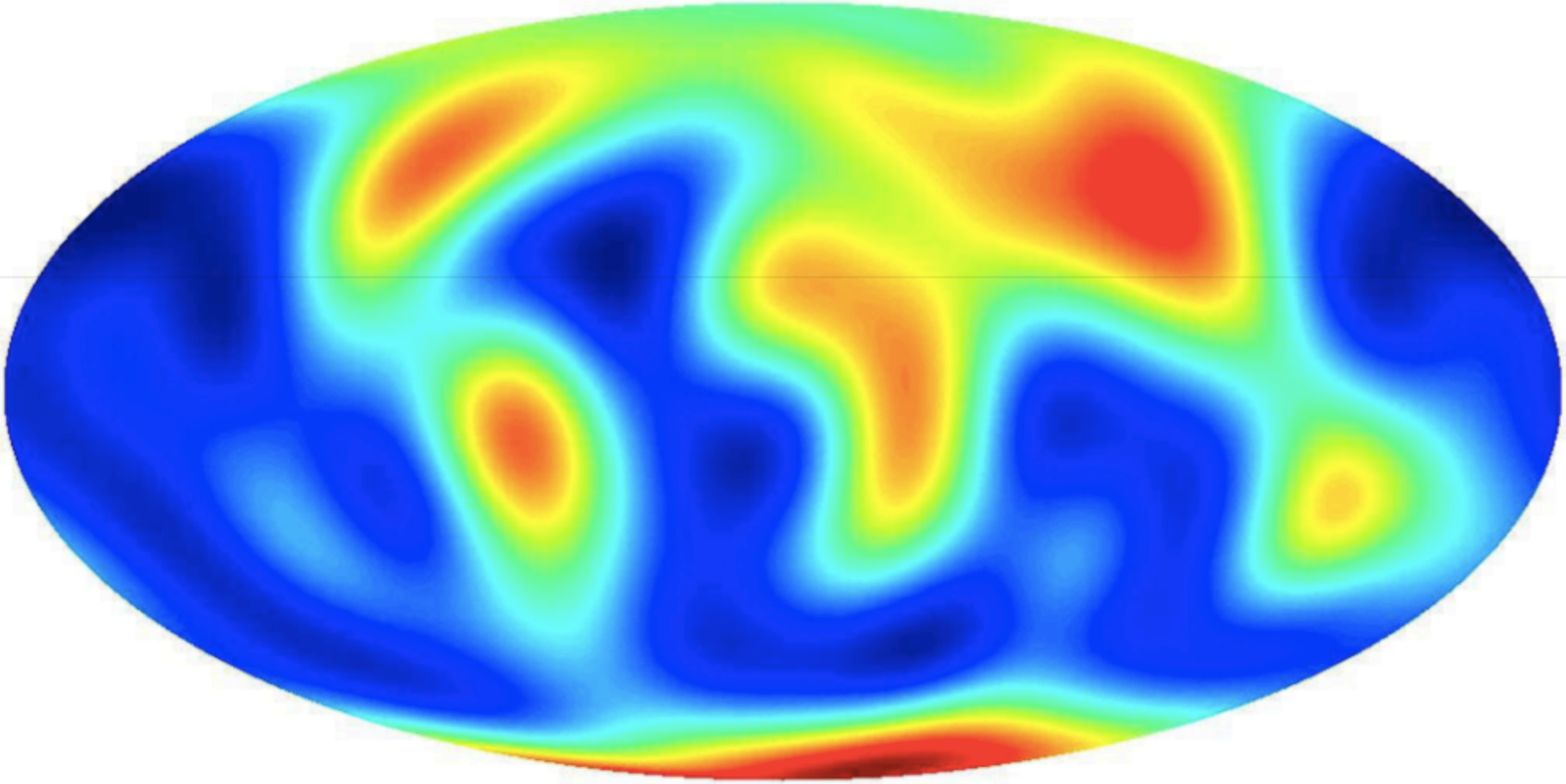

Made by Matthias Bartelmann

Sum up to some high ℓ

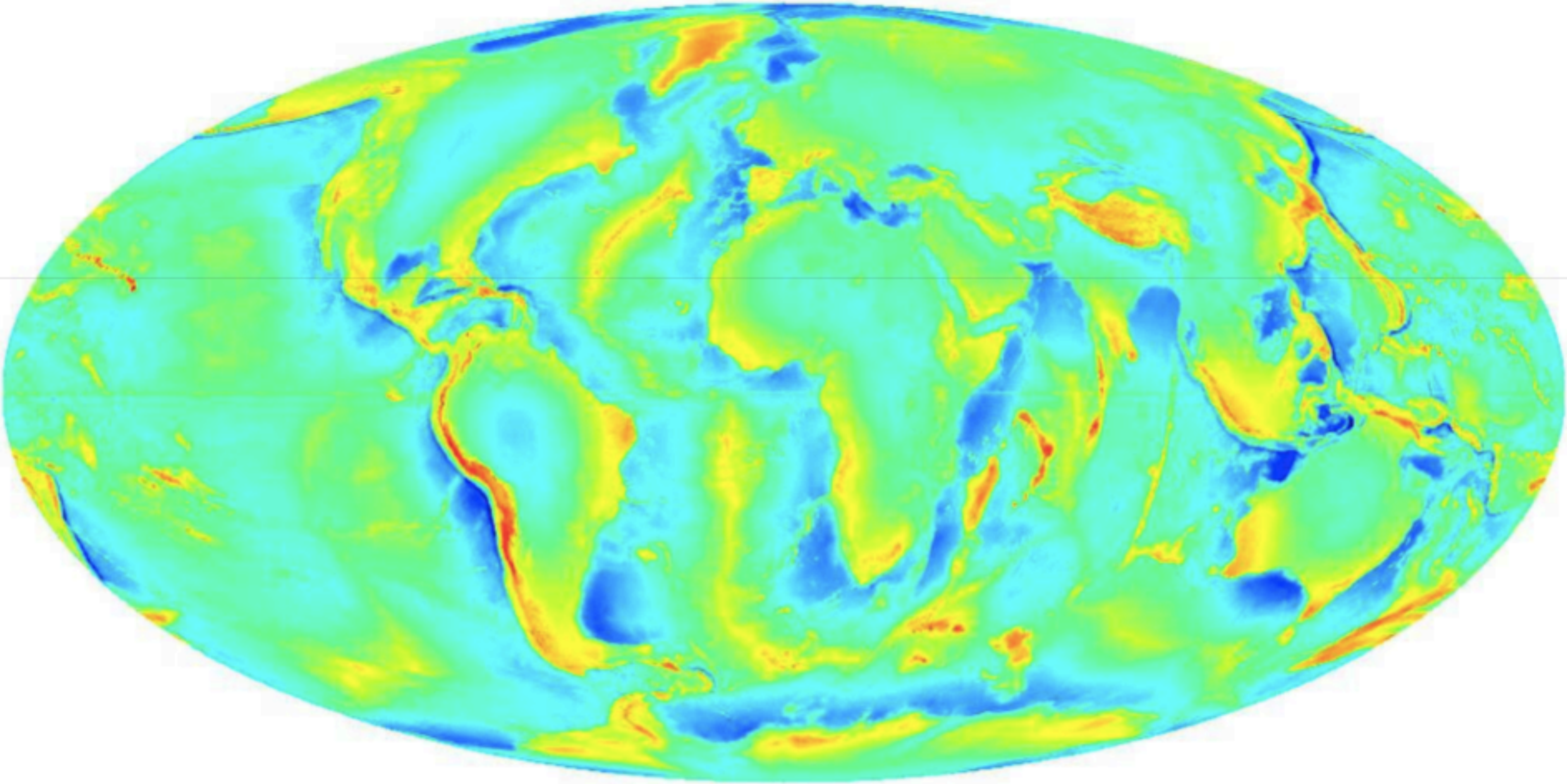

Made by Matthias Bartelmann

Map with all multipoles

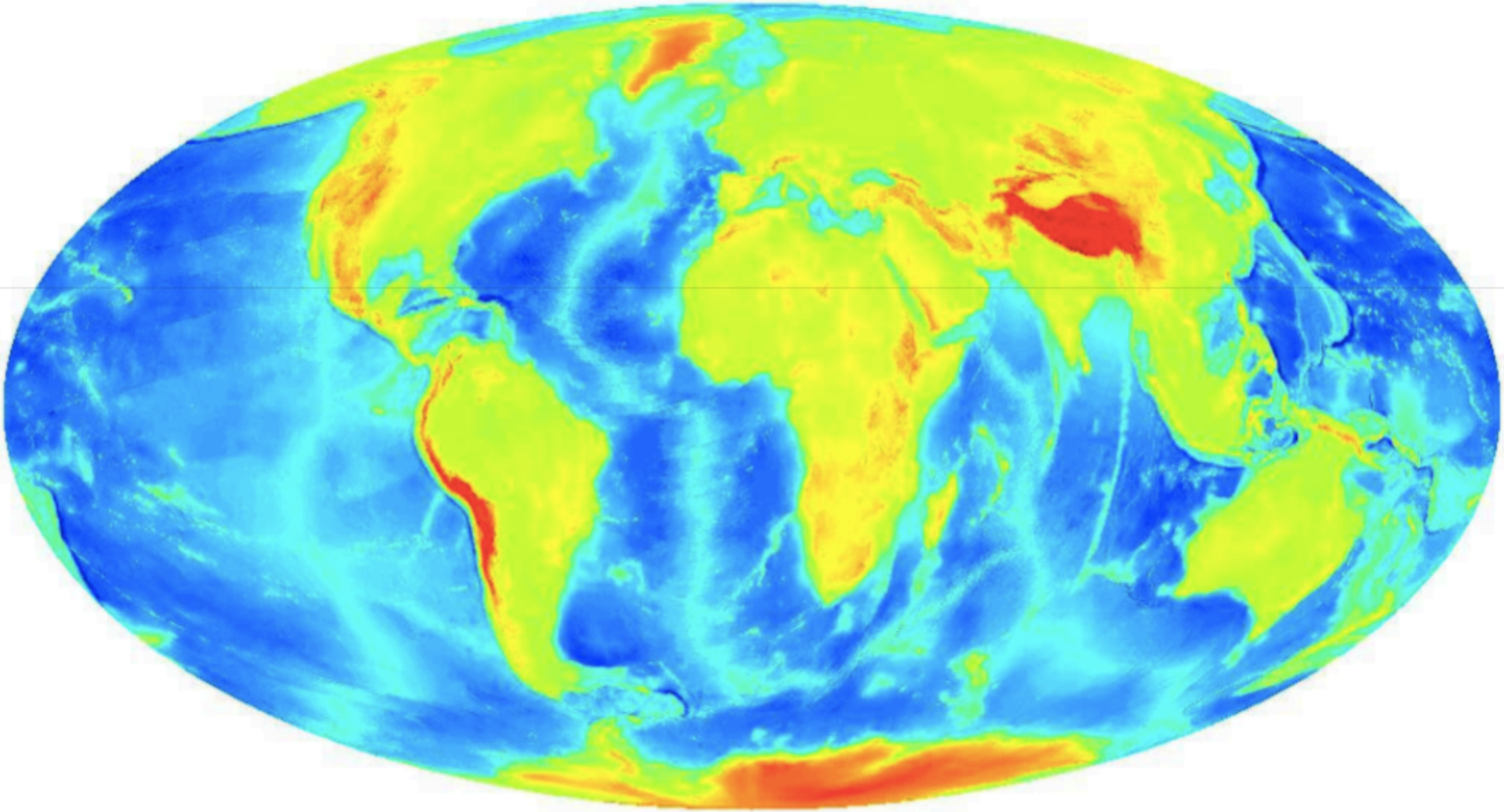

Angular correlation function

- the temperature fluctuation field is assumed as Gaussian Random variable. It's angular correlation function

$$C(\hat{n},\hat{n}') \equiv \left\langle \frac{\Delta T}{T}(\hat{n}) \frac{\Delta T}{T}(\hat{n}') \right\rangle = \sum_{\ell \, \ell'} \sum_{m \, m'} \langle a^*_{\ell m} a_{\ell' m'} \rangle \, Y^*_{\ell m}(\hat{n}) Y_{\ell' m'}(\hat{n}')$$

fully characterizes the temperature fluctuation field (brackets denote averages over an ensemble of Universes). It is conventional to write (the a_{lm} are not correlted):

$$\langle a^*_{\ell m} a_{\ell' m'} \rangle = C_\ell \delta_{\ell \, \ell'} \delta_{m \, m'} \quad , \quad C_l \equiv \left\langle |a_{\ell m}|^2 \right\rangle$$

C_l is the angular power spectrum. Then we have

$$C(\hat{n},\hat{n}') = \sum_\ell \frac{(2\ell+1)}{4\pi} C_\ell P_\ell(\cos\vartheta) = C(\cos\vartheta)$$

CMB angular power spectra

- temperature fluctuation spectrum:

$$\langle a^*_{\ell m} a_{\ell' m'} \rangle = C_\ell \delta_{\ell \ell'} \delta_{m m'} \quad , \quad C_l \equiv \left\langle |a_{\ell m}|^2 \right\rangle$$

- Polarization and cross correlation power spectra:

$$\left\langle E^*_{\ell m} E_{\ell' m'} \right\rangle = \delta_{\ell\ell'} \delta_{mm'} C_\ell^{EE},$$

$$\left\langle B^*_{\ell m} B_{\ell' m'} \right\rangle = \delta_{\ell\ell'} \delta_{mm'} C_\ell^{BB},$$

$$\left\langle \Theta^*_{\ell m} E_{\ell' m'} \right\rangle = \delta_{\ell\ell'} \delta_{mm'} C_\ell^{\Theta E}.$$

these quantities are highly sensitive to the cosmological parameters. They can be computed theoretically and measured from sky maps. Powerful tool to constrain cosmological parameters

CMB angular power spectra

Planck

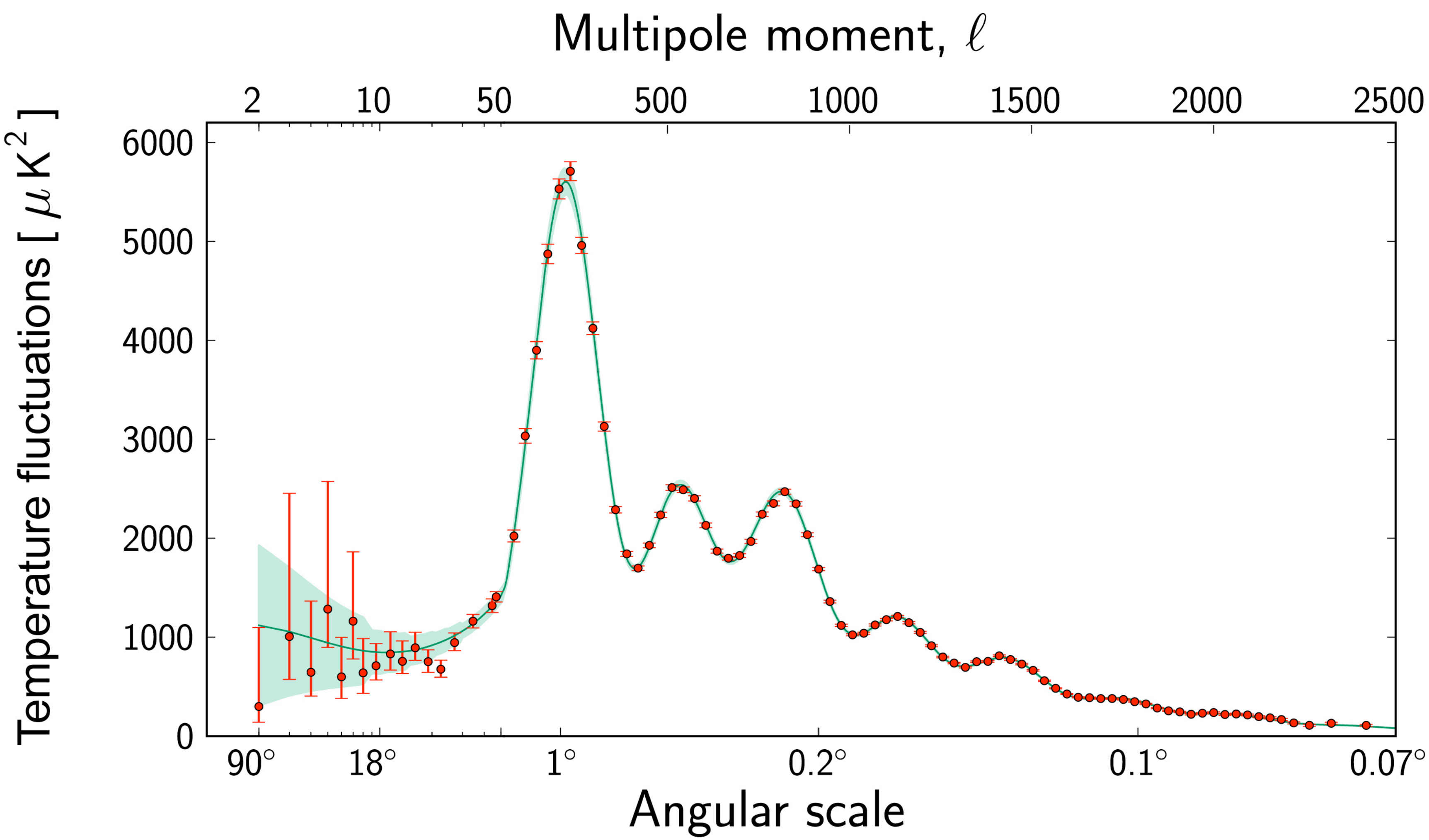

CMB angular power spectra

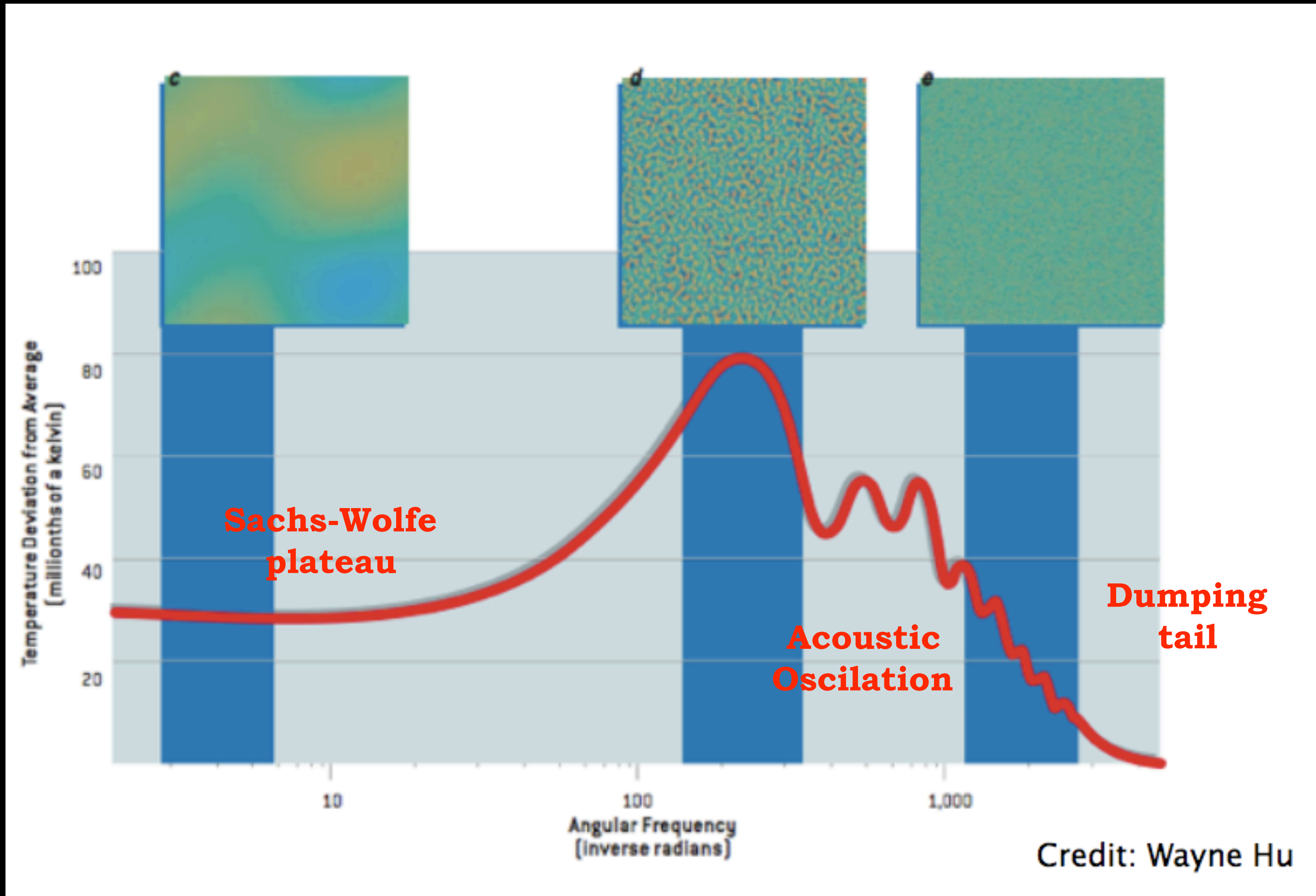

Sachs–Wolfe effect

$\Delta\nu/\nu \sim \Delta T/T \sim \Phi/c^2$

Additional effect of time dilation while potential evolves (White & Hu 1997):

$$\frac{\Delta T}{T} \sim \frac{1}{3}\frac{\Delta\Phi}{c^2}$$

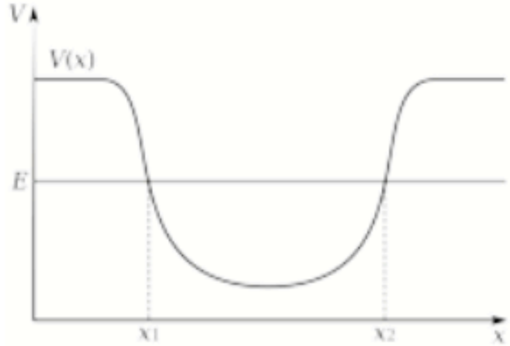

The temperature fluctuations due to the so-called Sachs–Wolfe effect are due to two competing effects: (1) the redshift experienced by the photon as it climbs out of the potential well toward us and (2) the delay in the release of the radiation, leading to less cosmological redshift compared to the average CMB radiation.

The first contribution leads to a redshift of the order of:

$$\frac{\delta T_1}{T} = \frac{\delta\Phi}{c^2}$$

Sachs–Wolfe effect

The second contribution is more tricky. Because of general relativity, the proper time goes slower inside the potential well than outside. The cooling of the gas in this potential well thus also goes slower, and it therefore reaches 3000 K at a later time relative to the average Universe.

The time delay (in terms of global time t) is:

$$\frac{\delta t}{t} = -\frac{\delta \Phi}{c^2} \tag{8.7}$$

This means that 3000 K is reached at a slightly larger (global) scale parameter $a + \delta a > a$. Since in the Einstein-de-Sitter Universe we have $a \propto t^{2/3}$ we can write

$$\frac{\delta a}{a} = \frac{2}{3}\frac{\delta t}{t} = -\frac{2}{3}\frac{\delta \Phi}{c^2} \tag{8.8}$$

Now, from that point $a = (a_{\rm cmb} + \delta a)$ until today $a = 1$ the redshift due to expansion is less by:

$$\frac{\delta z}{z} = -\frac{\delta a}{a} \tag{8.9}$$

which leads to a positive contribution to the temperature fluctuation δT that we observe today:

$$\frac{\delta T_2}{T} = -\frac{\delta z}{z} = \frac{\delta a}{a} = -\frac{2}{3}\frac{\delta \Phi}{c^2} \tag{8.10}$$

The total is the sum of both contributions:

$$\frac{\delta T}{T} = \frac{\delta T_1}{T} + \frac{\delta T_2}{T} = \frac{1}{3}\frac{\delta \Phi}{c^2} \tag{8.11}$$

Sachs-Wolfe effect

For power-law index of primary density perturbations (n_s=1, Harrison-Zel'dovich spectrum), the Sachs-Wolfe effect produces a flat power spectrum: $C_l^{SW} \sim 1/l(l+1)$

$$
\begin{aligned}
C_\ell &= \frac{1}{25}\int \frac{d^3k}{k^3}\mathcal{P}_\mathcal{R}(k) j_\ell(kx)^2 \\
&= \frac{4\pi}{25}\int_0^\infty \frac{dk}{k}\mathcal{P}_\mathcal{R}(k) j_\ell(kx)^2 \,, \qquad (67)
\end{aligned}
$$

the final result for an arbitrary primordial power spectrum $\mathcal{P}_\mathcal{R}(k)$.

The integral can be done for a power-law power spectrum, $\mathcal{P}(k) = A^2 k^{n-1}$. In particular, for a scale-invariant ($n=1$) primordial power spectrum,

$$\mathcal{P}_\mathcal{R}(k) = \text{const.} = A^2 \,, \qquad (68)$$

we have

$$C_\ell = A^2 \frac{4\pi}{25}\int_0^\infty \frac{dk}{k} j_\ell(kx)^2 = \frac{A^2}{25}\frac{2\pi}{\ell(\ell+1)} \,, \qquad (69)$$

since

$$\int_0^\infty \frac{dk}{k} j_\ell(kx)^2 = \frac{1}{2\ell(\ell+1)} \,. \qquad (70)$$

We can write this as

$$\frac{\ell(\ell+1)}{2\pi} C_\ell = \frac{A^2}{25} = \text{const. (independent of } \ell) \qquad (71)$$

Acoustic oscillations

- Baryons fall into dark matter potential wells: Photon baryon fluid heats up
- Radiation pressure from photons resists collapse, overcomes gravity, expands: Photon-baryon fluid cools down
- Oscillating cycles on all scales. Sound waves stop oscillating at recombination when photons and baryons decouple.

Credit: Wayne Hu

Springs: photon pressure

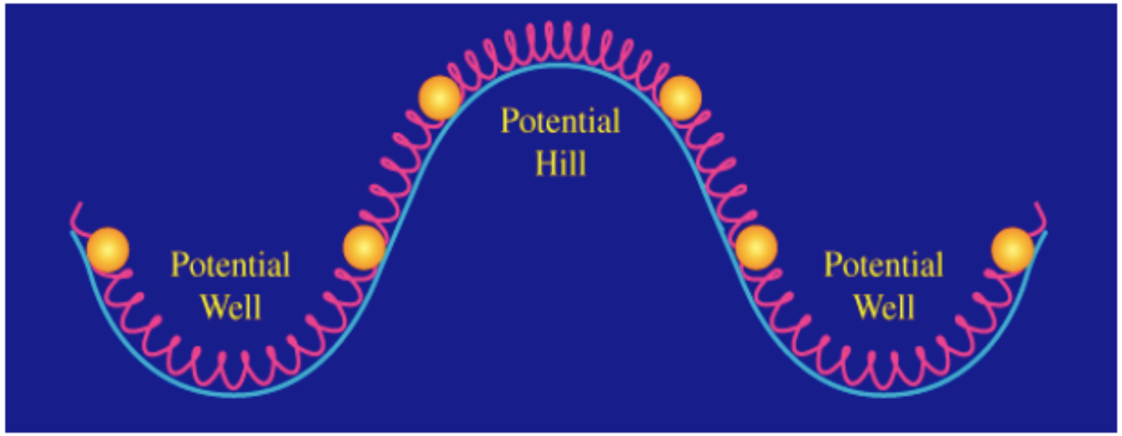

Balls: baryon mass

Acoustic peaks

Oscillations took place on all scales. We see temperature features from modes which had reached the extrema

- Maximally compressed regions were hotter than the average
  Recombination happened later, corresponding photons experience less red-shifting by Hubble expansion: HOT SPOT

- Maximally rarified regions were cooler than the average
  Recombination happened earlier, corresponding photons experience more red-shifting by Hubble expansion: COLD SPOT

Harmonic sequence, like waves in pipes or strings:

2nd harmonic: mode compresses and rarifies by recombination
3rd harmonic: mode compresses, rarifies, compresses

➡ 2nd, 3rd, .. peaks

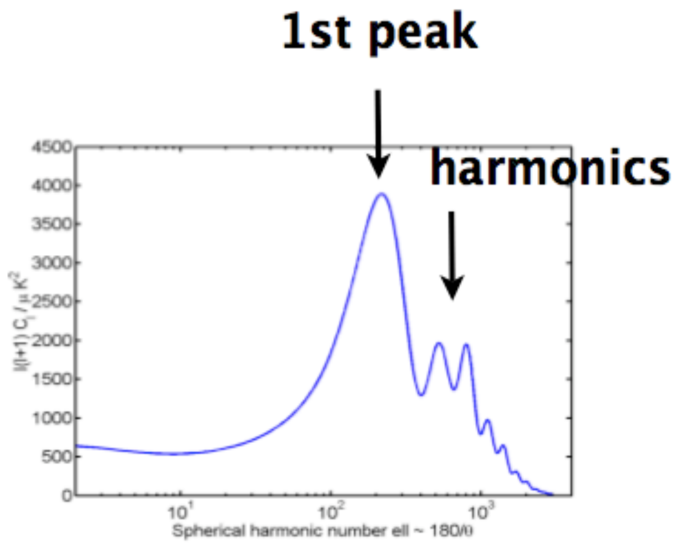

Harmonic sequence

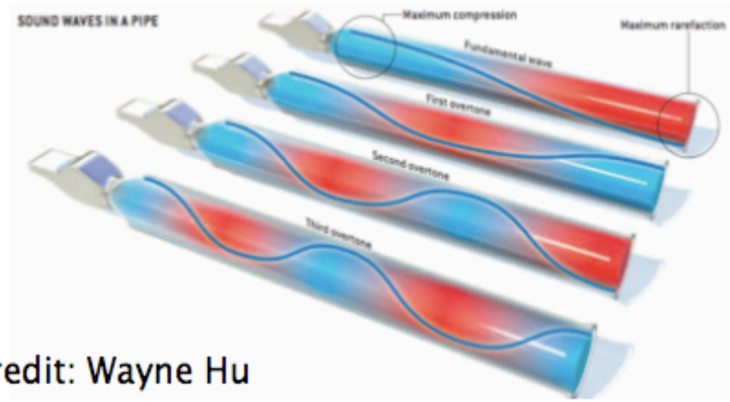

Credit: Wayne Hu

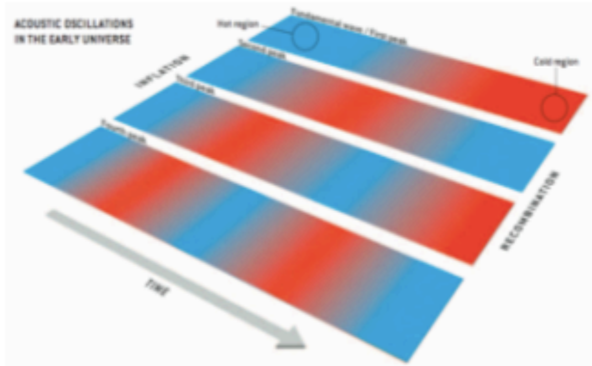

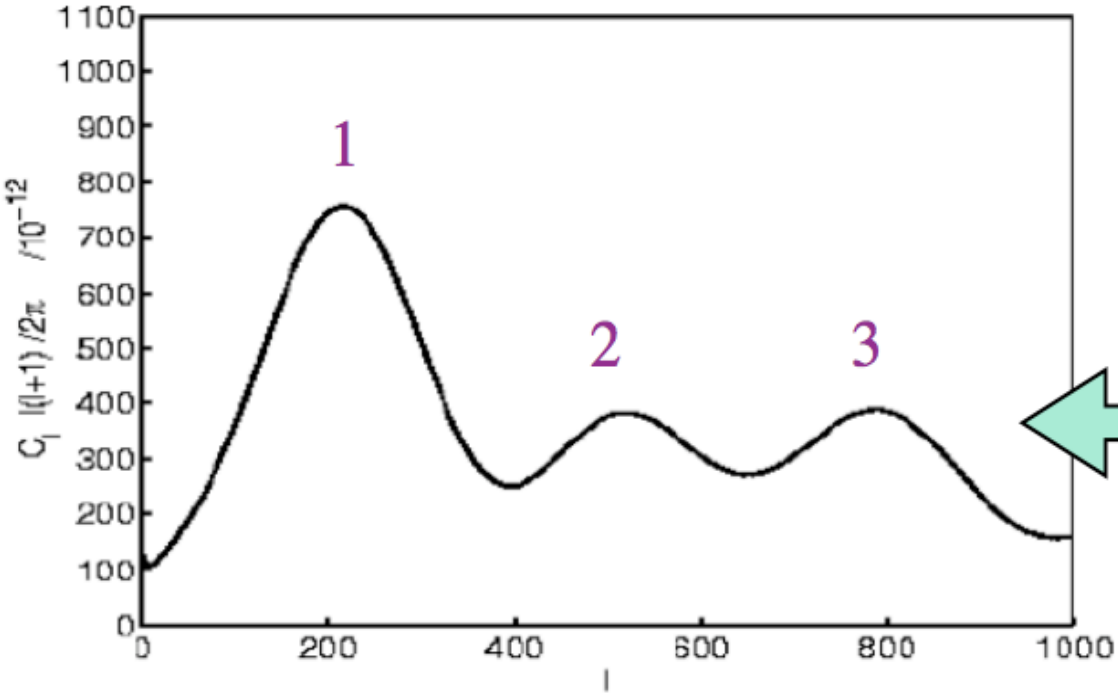

Modes with half the wavelengths osccilate twice as fast ($\nu = c/\lambda$).

Peaks are equally spaced in ℓ

Doppler shifts

Times in between maximum compression/rarefaction, modes reached maximum velocity

This produced temperature enhancements via the Doppler effect (non-zero velocity along the line of sight)

This contributes power in between the peaks

➡ **Power spectrum does not go to zero**

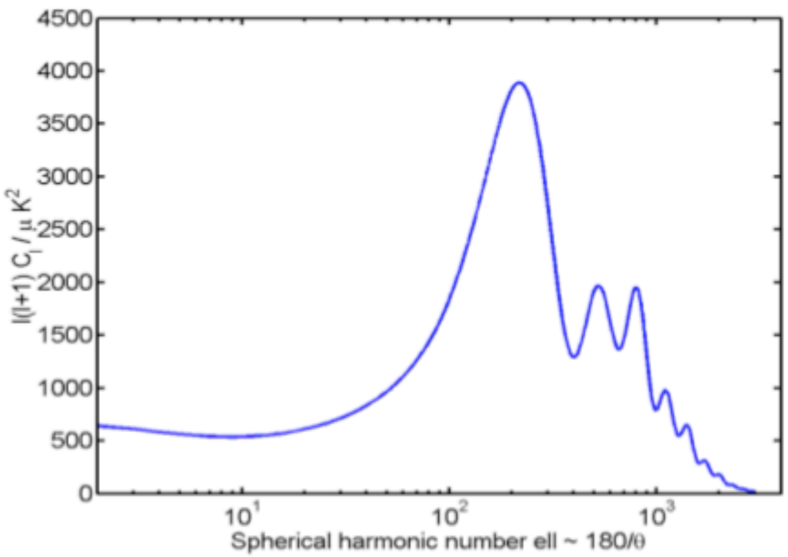

Damping and diffusion

- Photon diffusion (Silk damping) suppresses fluctuations in the baryon-photon plasma

- Recombination does not happen instantaneously and photons execute a random walk during it. Perturbations with wavelengths which are shorter than the photon mean free path are damped (the hot and cold parts mix up)

This is same as a low-resolution instrument blurs all the details!

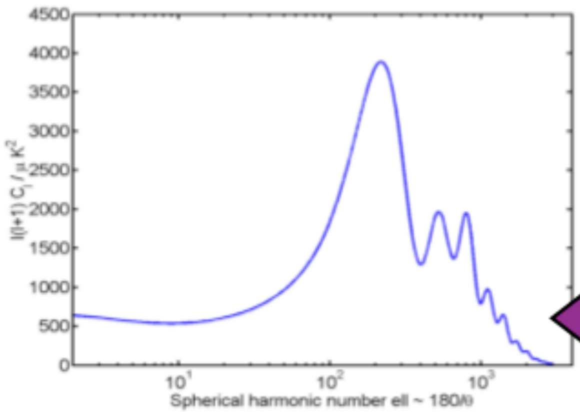

Power falls off

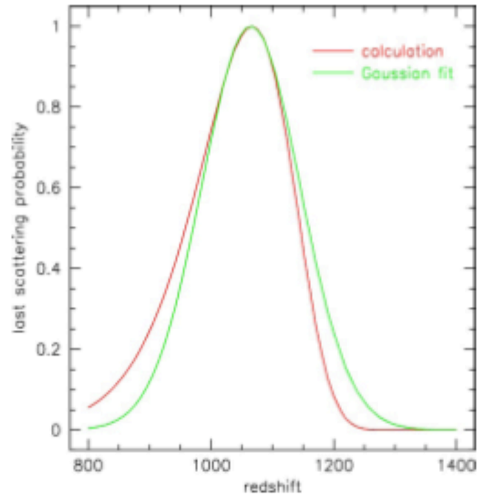

Thickness of the LSS is comparable to the oscillation scales

CMB angular power spectra

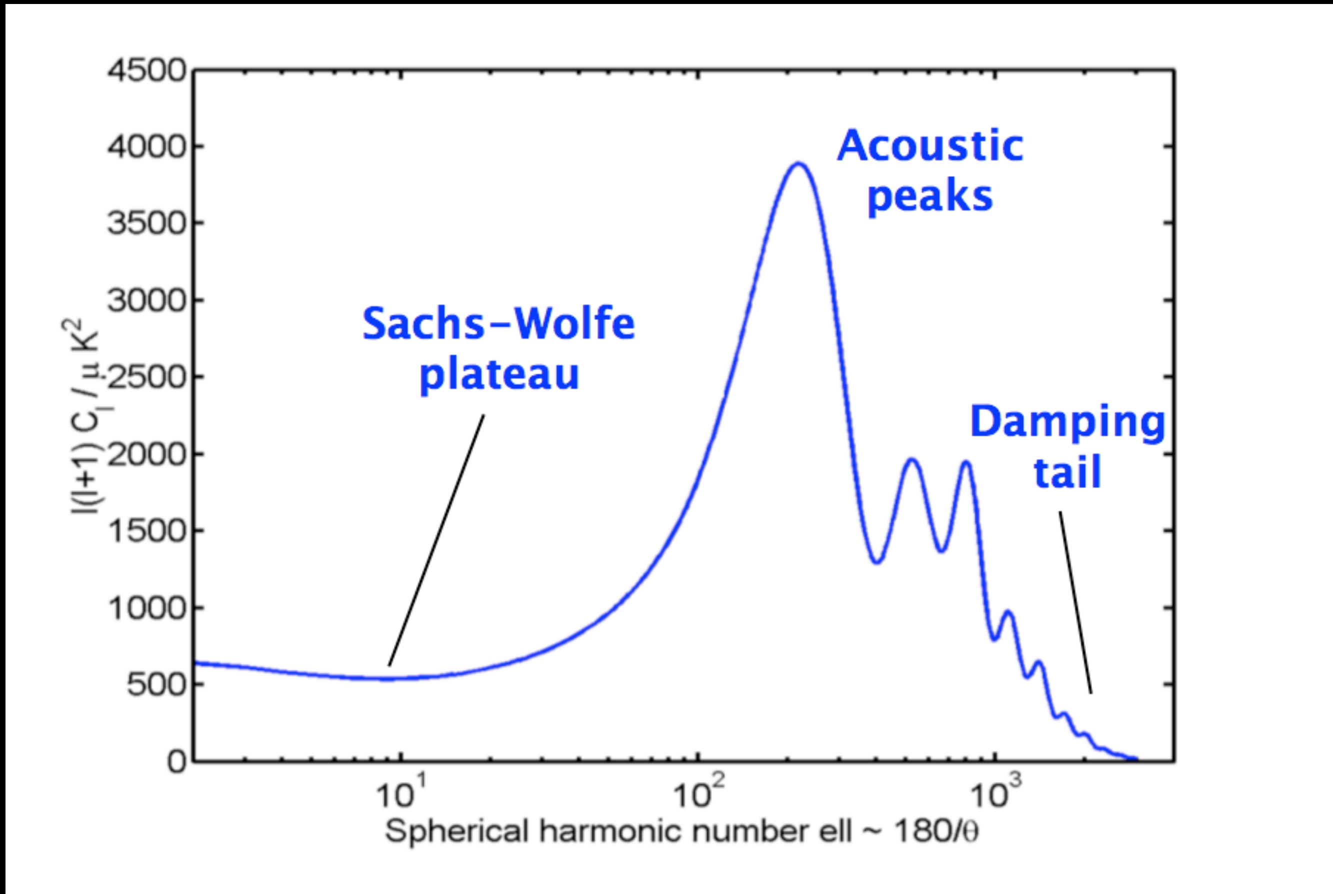

Online C_l calculators

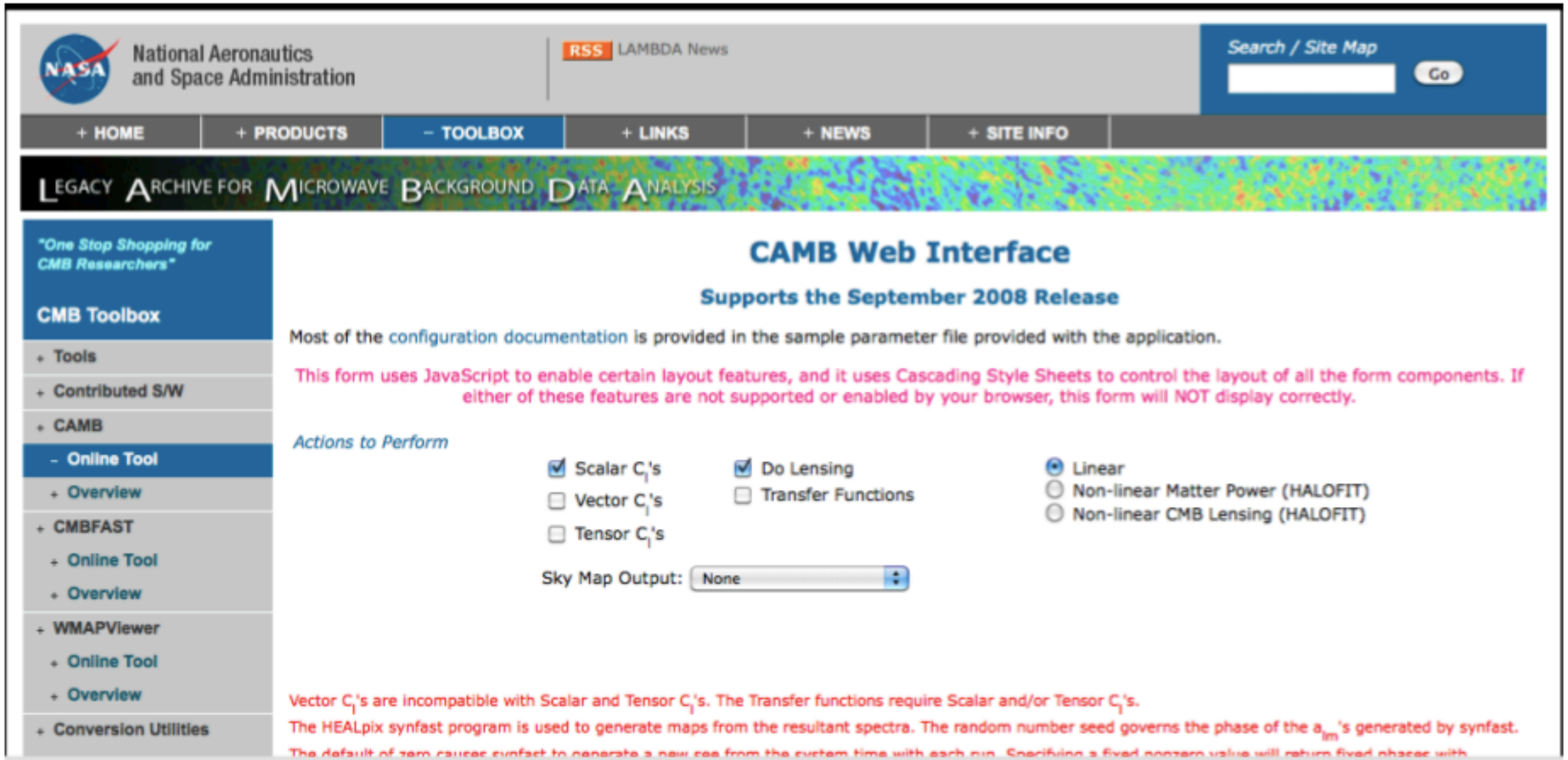

CMB Toolbox: http://lambda.gsfc.nasa.gov/toolbox/

CAMB website: http://camb.info/
CMBFast website: http://www.cmbfast.org/

temperature power spectrum: parameter dependence

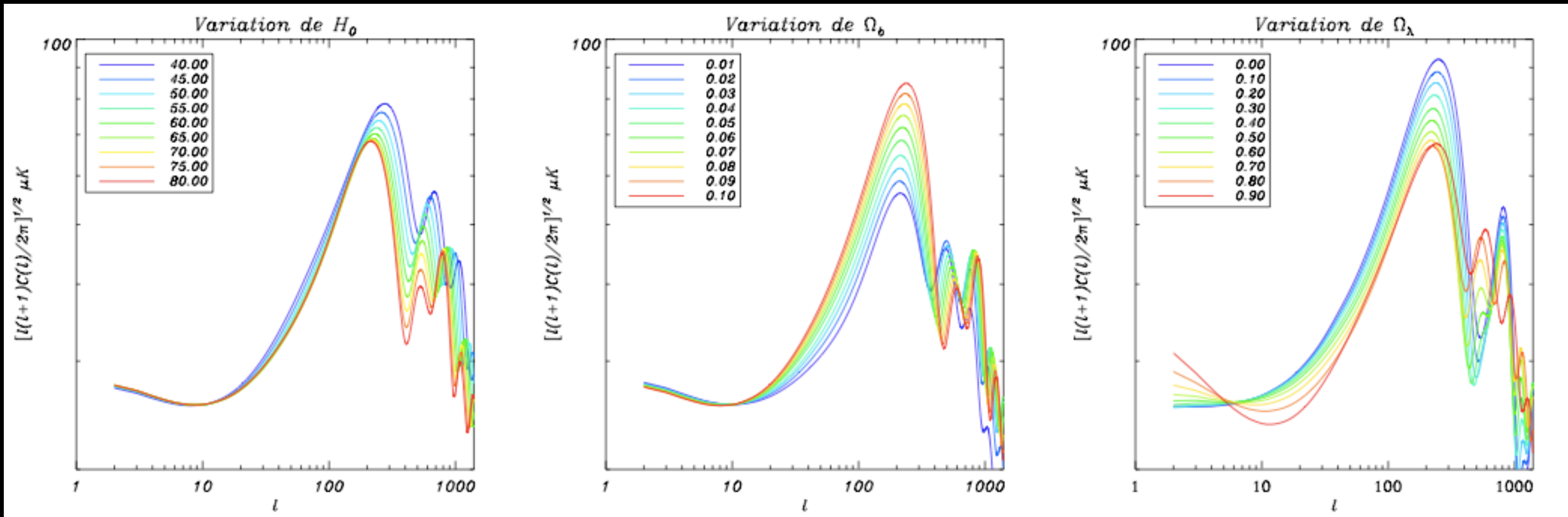

There are model degeneracies among parameters.

CMB parameter cheat sheet